2024

Functionalizing silicon oxide like surfaces with fatty acids

Maman Sani Maman Brah Maman

FUNCTIONALIZING SILICON OXIDE LIKE SURFACES WITH FATTY ACIDS

Maman Sani Maman Brah Maman

A THESIS

Submitted in partial fulfillment of the requirements
for the degree of Master of Science
in
Chemistry
to
The Graduate School
of
The University of Alabama in Huntsville
May 2024

Approved by:

Dr. Jeffrey Weimer, Research Advisor & Committee Chair
Dr. Carmen Scholz, Committee Member
Dr. Bernhard Vogler, Committee Member
Dr. Bernhard Vogler, Department Chair
Dr. Rainer Steinwandt, College Dean
Dr. Jon Hakkila, Graduate Dean

Abstract

Functionalizing Silicon Oxide Surfaces with Fatty Acids

Maman Sani Maman Brah Maman

A thesis submitted in partial fulfillment of the requirements for the degree of Master of Science

Chemistry

The University of Alabama in Huntsville
May 2024

The goal of this project was to make flat hydrophilic, silicon oxide-like surfaces hydrophobic. Using fatty acids in a wet chemistry approach, glass, mica, and silicon wafer surfaces were cleaned with standard methods from the literature. The substrates were functionalized with oleic acid and stearic acid in ethyl alcohol. The solution concentration was held constant at 100 times a theoretical minimum concentration. The substrates were immersed at various functionalization times and various solution temperatures. Contact angle goniometer was used to measure the contact angle for water on the functionalized surfaces. The results confirmed that glass and oxidized silicon wafer surfaces can be made hydrophobic with oleic or stearic acid. The optimal immersion time in oleic acid was 1,000 min. At longer times, the surfaces become hydrophilic again. Functionalizing with stearic acid gave comparable contact angles to oleic acid for room temperature and 80 °C. Contact angles for oleic acid were lower at intermediate temperatures. The observations were proposed to be due to a bilayer formation at higher acid concentration.

Acknowledgements

I am grateful to my advisor Dr. Jeffrey Weimer, for all his help, guidance, mentoring, suggestion, and correction from day one upon joining his research group. I would also like to thank Dr. Bernhard Vogler and Dr. Carmen Scholz for their useful suggestions and insightful comments.

I would also like to thank Leanne, Noah, Madison, Anna, Taba, Ouani, the Alexanders, and the Hamissous for their love, help and supports. I would not finish without thanking all my family and friends for being on my side from day one.

Table of Contents

List of Figures

List of Tables

List of Symbols

Symbol	Description
$l_{C=O}$	The radius of the carbonyl C=O ($l_{C=O}$) (m)
l_{C-O} (m)	The length of the carbon-oxygen (l_{C-O}) (m).
l_{C-C} (m)	The length of the carbon -carbon (l_{C-C}) (m).
r_m (m)	The exclusion radius r_m (m) along the surface.
Cm	The theoretical minimum concentration (μM).
$\rho NoA = \frac{1}{A}$	The number density of molecules per unit area (molecules /cm^2).
$N_1 = \frac{1}{A}$	The number of molecules to cover 1 cm^2 area.

Chapter 1. Introduction

1.1 Research Goal

The goal of this project is to functionalize hydrophilic silicon oxide-like surfaces such as glass, mica, and silicon (Si) wafers to become hydrophobic to the greatest degree possible. A surface is hydrophobic when its water contact angle is above 90°, and surfaces with water contact angles below 90° are hydrophilic. Surfaces with water contact angles above 150° are called super hydrophobic.[1]

1.2 Foundations

1.2.1 Functionalizing Surfaces

Functionalization can be defined as the process of modifying the surface of a material by inducing fundamental biological, chemical, or physical changes to make it have a different behavior. We can list representative examples for where functionalization is beneficial in an application. Examples of inducing fundamental biological changes include coating bones with biopolymers or bioactive materials for bone regeneration,[2,3] or coating the surfaces of medical implants devices with organic acids to make them suitable for implants and drug delivery systems.[4,5] For chemical applications, examples include engineered nanomaterials for environmental applications,[6] carbon based adsorbents surfaces modified for carbon dioxide (CO_2) capture,[7] and radio nuclide removal.[8] Other examples include sol-gel coating or dip coating used in manufacturing thin films in coating industries.[9–11] Organic acids and silanes are applied on material

surfaces to enhance the adhesion of coatings and improving their durability.[12,13] Chemical applications also include laser transmission welding and surface modification of graphene film for flexible supercapacitor applications,[14] super hydrophobic coating of airplane wings to resist icing,[15] anti-reflective coatings to lenses and screens to reduce glare and reflections,[16] anti-reflective coatings used in solar panel cells to increase performance and durability.[17] Finally, applications that use physical modification include glass micro-spheres in tall building windows and thermal insulation materials used in aerospace and ships.[18,19]

1.2.2 Silicon Oxide-Like Surfaces

Silicon oxide like surfaces are found on pure silicon dioxide (SiO_2 or quartz), oxidized surfaces of silicon (Si) wafers, glass, and mica, ($KAl_2AlSi_3O_{10}(OH)_2$). Silica, an amorphous and often porous form of SiO_2, is a useful support for catalysts.[20] Silicon dioxide is used in manufacturing capacitors and transistor as an insulator layer to isolate various elements.[21] Oxidized porous silicon is used for biosensing application.[22] Glass has application in drinking glassware, bottles, cookware, architectures, laboratories, electronic technologies, and manufacturing.[23] Mica has application in cosmetic, construction, electronics, automotive, and painting.[24]

The chemistry and structure of silicon oxide like surfaces are generally the same.[25] The silicon atoms primarily have a complete tetrahedral configuration.[26] The free valency of surface silicon atoms becomes saturated with hydroxy groups (≡Si–OH) in an aqueous solvent.[27] Silicon oxide like substrates can therefore be hydrophobic[26] because they are mostly composed of silanol groups and siloxane groups (OH).[20,27] Pure quartz is atomically flat. Quartz has a body-centered tetrahedral crystal system composed of SiO_4

tetrahedra. The structure includes a central silicon atom bonded to four oxygen atoms, with one oxygen atom bonded to two silicon atoms. The O-Si-O bond in one tetrahedron forms a 109° angle, while the Si-O-Si bond in the networked SiO_4 tetrahedra makes a 144° angle. The open structure of networked SiO_4 creates wide spaces, to give quartz its hexagonal crystalline form.[26] Surfaces of oxidized silicon wafers and glass mimic the same chemistry. Silicon wafers surfaces have the same smoothness as glass.[25,28] Glass has amorphous structure adds disorder to the structure of the network, and may have modifiers in it.[23,29–31] Mica has crystalline structure and has additional chemistries in it, such as potassium and aluminum.[25] Mica surfaces are also atomically flat and smooth therefore ideal for attaching molecules and depositing gold films.[25,28]

Silicon oxide like surfaces have been functionalized for various applications. Biological examples include immobilization of biomolecules on glass with self-assembled monolayers (SAMs) in order to create DNA chips and protein microarrays for genotyping, gene-expression profiling, and diagnostic biomarker identification.[32] An additional application is the modifications of bioactive glasses to generate a biological response to cells on outermost surface layer.[32] Silicon oxide like surfaces will readily react with carboxylic group of organic groups (OH).[27,33,34] Chemical examples include using wet chemical to assemble organic monolayers on silicon surfaces via the formation of Si–C bonds.[35] Another example is the functionalization of silicon wafer with luminescent Tb(III) coordination complex for the optical detection of NO in the gas phase.[36] Physical modifications include roughening microfiber glass surfaces to use in windows for insulation and keeping them cleaned.[18,19]

1.2.3 Organic Acids

Organic acids, mainly fatty acids, can be saturated (no double bonds) or unsaturated (containing double bonds).[37] Saturated fatty acids are typically solid at room temperature, while unsaturated ones with the same chain length are often liquid at room temperature. As shown in Figure 1.1, stearic acid (SA, octadecanoic acid, $CH_3(CH_2)_{16}COOH$) with a saturated molecular structure has the same chain length as unsaturated oleic acid (OA, (9Z)-octadec-9-enoic acid, $CH_3(CH_2)_7(CH)_2(CH2)_7$- COOH). The unsaturated organic acid can have a cis or a trans double bond.[37] The trans and cis molecular structure configurations display two different molecular shapes for the same organic acid. Oleic acid with the trans molecular configuration is shown in Figure 1 (b) on the next page. It has a linear molecular shape structure. The cis molecular structure configuration in Figure 1 (c) on the next page shows that the cis- double bond creates a kink in the chain. The kink affects the shape of the molecule therefore affects the molecule properties. Literature reported that the presence of the kink in the structure affects the melting point,[37] with cis OA melting at a lower temperature than trans OA.

Organic acid molecules are amphiphilic because they are composed of a carboxyl functional group (-COOH) at one end and an aliphatic hydrocarbon chain R at the other. The aliphatic hydrocarbon chain is nonpolar and makes the acid molecule hydrophobic, while the carboxyl group (COOH) is polar and hydrophilic. The carboxyl group participates in chemical reactions such as esterification to form triglycerides (fats and oils) or amidation to form proteins,[38,39] with acids linked through condensation reaction resulting in a loss of the hydroxyl (OH) group from one acid and a proton from the second acid. A water molecule is formed in the process, and the two acids are linked

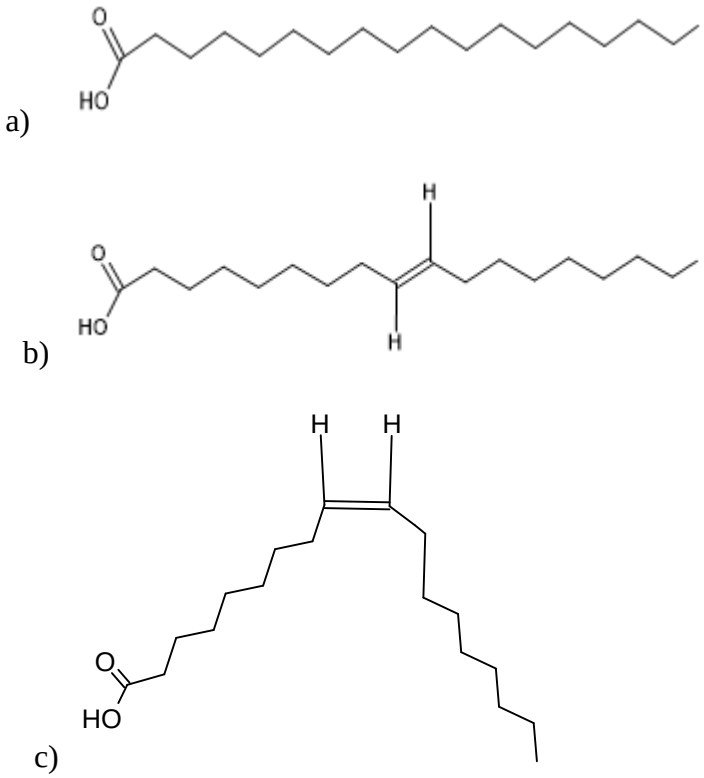

Figure 1.1 Structures of organic acids. a) Saturated stearic acid with no double bond. b) Trans configuration of oleic acid. c) Cis configuration of oleic acid displaying the kink of the structure.

through an amide or peptide bond. The carboxylic end of organic acids also makes them candidates for surface modifications.[40]

Unsaturated organic acids, such as omega-3 and omega-6 fatty acids, have important roles in human health.[41] They are considered essential because the body cannot synthesize them and must obtain them from diet. Organic acids react with bases to form soap through the process of saponification.[42] Organic acids are also insoluble in water but soluble in organic solvents such as hexane, ethyl alcohol, n-decane, and benzene. The melting point of organic acids depends on the R chain length. The melting point increases with the chain length and decreases with the degree of saturation.[35]

1.2.4 Reacting Organic Acids with Silicon Oxide-Like Surface

The chemical process for adsorption of an acid molecule on a silicon oxide-like

surface starts with the proton of the carboxyl group of the acid forming a hydrogen bond with the oxygen of the silanol group of the surface.[20,27,33,43,44] The mechanism is shown in Figure 1.2a and 1.2b on the next page. The chemistry of organic acids functionalizing silicon like oxides surfaces is an esterification reaction. The carboxyl group (COOH) of the acid is the reaction site for the adsorption inter-action between the surface of the silicon oxides and the acid molecule.

1.3 Previous work

Oleic acid was used to functionalize glass substrates composed of soda-lime-silicate, silica slide glasses, and a soda-silicate glass.[44] The solvent, the organic acid, the temperature, and the functionalization time were held constant. The glass substrates were washed with acetone, then rinsed with ethyl alcohol and dried in vacuum for 24 h. Soda-silicate glass containing 12 mol % Na_2O was fabricated by a melting process in a furnace. The substrates were ground and stored in a desiccator. A mass of 0.5 g of the powder samples was mixed with reagent ethyl alcohol, and 0.1 mL of OA was added to the mixture. The exact acid concentration was not provided in the work. The mixture was left to react for 24 h, separated, and centrifugated for 20 min. The sediment layer part of the mixture was dried in a vacuum for 24 h and stored in a desiccator.

Diffuse reflectance infrared Fourier transform spectroscopy (DRIFTS) was used for analysis. Analysis revealed a correlation between the structure, composition, and dissolution properties of the glasses and the coating properties of OA. Bonding mechanisms between the OA and the glass surface were also identified. Metal ions on the soda lime–silicate glass surface produced metal-(Na+, $Ca^{2+,}$ and Al^{3+}) oleates through the formation of metal– carboxylate complexes. Partial dissociation of the OA

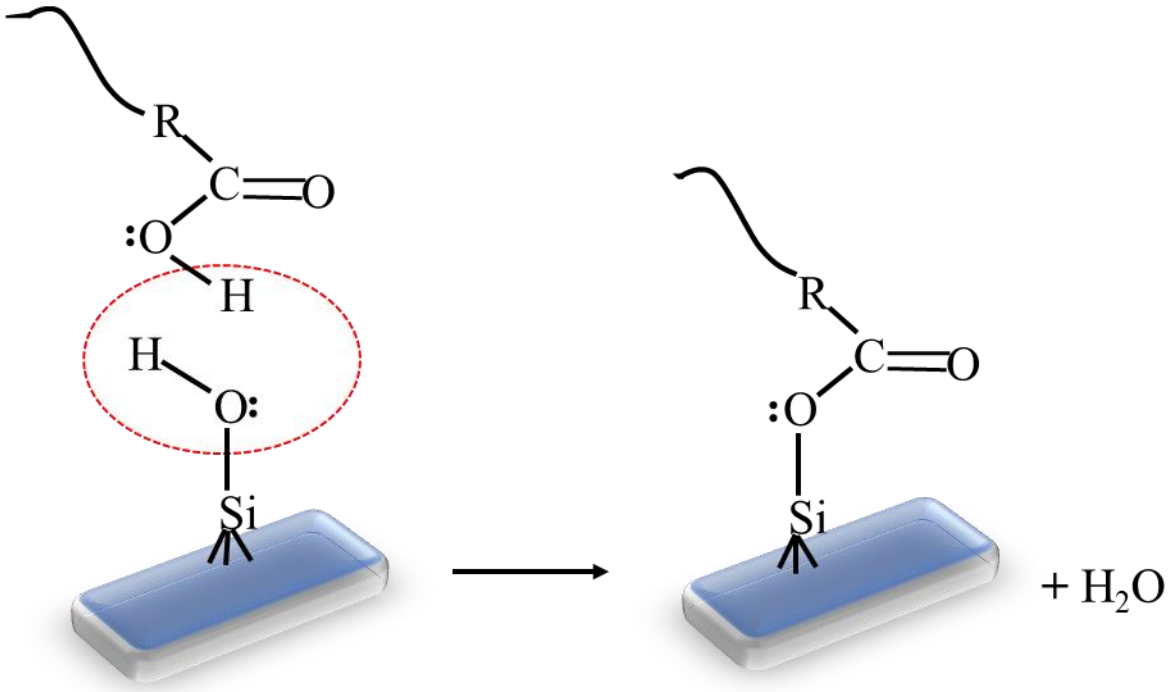

Figure 1.2a Schematic representation of the chemical reaction of oleic acid adsorption process on a silicon oxide-like surface. After a hydrogen bond is formed, another interaction is engaged between the proton (H) of the carboxyl group trying to form a bond with the oxygen of the silanol group of the surface. Consequently, water is removed with condensation through esterification reaction.

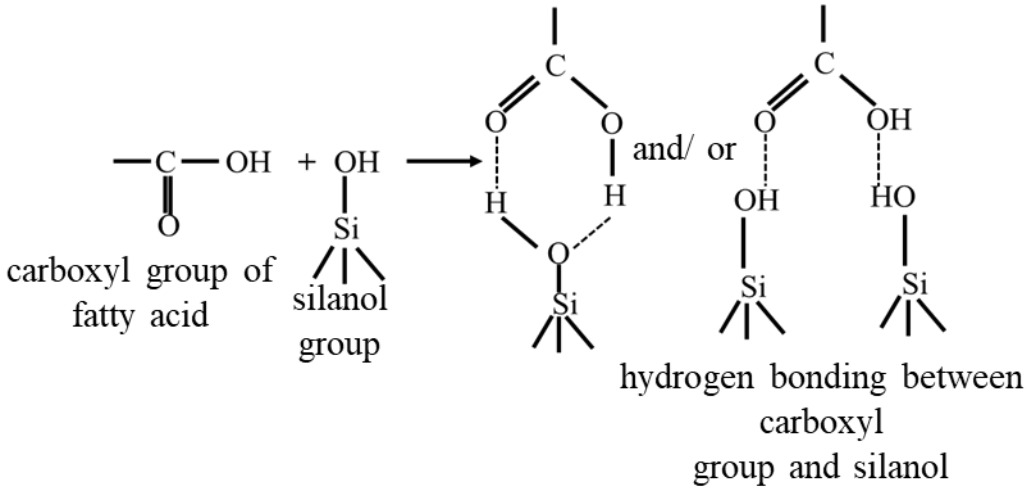

Figure 1.2b Interaction mode between the surface silanol group and the carboxyl group of the organic acid. A simultaneous hydrogen bonding formation occurs between the proton of the silanol group of the surface with the oxygen of the carbonyl group. Meanwhile, the hydrogen bond is formed between the proton of the carbonyl group with the oxygen of silanol.

was observed on soda-lime silicate glasses. The OA dissociated completely on soda-silicate glass. Only hydrogen bonds were formed with OA and silanol groups on the surface of silica glass substrate.

Silica glass was used as a substrate to functionalize with acid[45] (rosa canina). The substrate (silica glass), type of fatty acid (rosa canina), temperature (37 °C), functionalization time (3 h) were held constant. The initial concentration of acid was 10 mg/ mL and was varied, but no details of the variation were provided. The substrates were cleaned in an acetone ultrasonic bath for 5 min and rinsed with water. Fluorescence microscopy and x-ray photoelectron spectroscopy (XPS) were used for characterization. The results showed changes in the morphology of the substrate surface, particularly changes on the substrate roughness and also indication of biomolecule grafting from the changes of the acid concentration.

Mica has less reactive groups on its surface and reportedly cannot be functionalized using chlorosilanes.[46] Mica and calcite substrates have however been functionalized by SA, OA, 18-phenoloctadecanoic acid (PODA), and 18-cyclohexyloctadecanoic acid (CHOA) in n-decane[43]. The substrates (mica and calcite), methods (wet and dry), organic acids (OA, SA, PODA, CHOA) were varied while functionalization time (20 h), the solvent (n-decane), and concentration (0.01 M) were held constant. In the dry method, the solid surfaces were dried for 4 h at a temperature of 150 °C under nitrogen flow before the acid functionalization. The liquid (n-decane) was dried overnight over molecular sieves (0.04 Nm). For the wet modification, the dried solid surfaces were placed in a desiccator in the presence of a saturated solution of K_2SO_4 for 10 days. The solution was kept at room temperature. For the two types of

modifications, a 0.01 M solution of each acid in n-decane was prepared. The samples were stirred with a slowly rotating agitator (45 rpm) for 20 h. After centrifugation, the mixture was dried.

Thermogravimetric analysis, vapor adsorption isotherm, and microcalorimetric enthalpy of adsorption of water were used for characterization. The results showed two key factors. The surfaces of the substrates and the molecular structures of the organic acids play a role in the organic acids adsorption process. For calcite, both parallel and perpendicular adsorption orientations of molecules occurred depending on the structure of the long chain fatty acids. Saturated aromatic ring CHOA had parallel adsorption. The saturated SA, the saturated PODA, and unsaturated OA had perpendicular adsorption. All the organic acids exhibited a parallel adsorption orientation on the surface. Finally, the adsorption of organic acids was reported to be stronger on calcite than on mica.

Silicon oxides nanoparticles modified by oleic acid were prepared using wet chemistry surface modification method.[20] The work studied the effects on coverage and dispersion of SiO_2 nanoparticles in oil by OA with variations of concentration and temperature. A mixture of n-hexane, OA, and an appropriate amount of the nanoparticles (no specific concentration was provided) was heated at 60 °C under vigorous stirring for 4 h. After filtration, the sediment was rinsed with ethyl alcohol and then with dI water. The precipitate was kept for 24 hours in a vacuum desiccator. The work was repeated by changing the concentrations ratio of OA to SiO_2, the reaction temperatures from 50 °C to 80 °C and the solution solvents (n-hexane, plasticizer, water, tetrachloromethane (CCl_4), and ethyl alcohol).

Fourier transform infrared spectroscopy (FTIR), transmission electron microscopy

(TEM), and XPS were used to characterize the samples. The analysis focused on before and after the surface modification. The OA-modified SiO_2 nanoparticles were found to disperse steadily in mineral oil. Esterification was proposed to bond the OA to the surface of the SiO_2 nanoparticles. An ideal reaction temperature and an ideal ratio of OA to SiO_2 were determined to be 60 °C and 20%, respectively. The FTIR results also provided evidence that not all the silanol groups on the surface were reacting in the process. Further analysis also showed the existence of both carboxylate and silanol. The reaction was described as below:

$$SiO_2(OH)_n + yHOOCC_{17}H_{33} \longrightarrow SiO_2(OH)n\text{-}y(HOOCC_{17}H_{33})y + H_2O \quad (1.2)$$

Reactive force field (ReaxFF) molecular dynamics simulation was used to determine the adsorption mechanism of OA on the surface of aluminum (Al) nanoparticle.[47] The concentration of OA on the Al nanoparticles was changed gradually from the initial density of 0.05 g/ cm^3. The OA molecules adsorbed at the carboxylic groups to form carboxylates. A single chemical monolayer was formed. As the acid density increased, the monolayer was proposed to become a bilayer due to the increase of the acid concentration. The increase in the acid molecules carboxylic groups created inner and outer layers of carboxylic ends stacked on top of each other. The stacking of the carboxylic groups trapped the aliphatic ends and rendered the bilayer to be spherical in shape. The findings were confirmed by FTIR and XPS.

A relationship has been reported between molecular structures of organic acids absorbed on a surface and the friction coefficients of the surface.[37] Monolayer films of OA and SA on iron- oxide surfaces lubricated by squalane over adsorption times of 24 hours. N-hexadecane was used as solvent for both OA and SA to produce films of

3.5-4.5 nm of thickness under static and shear conditions. Sum frequency spectroscopy and polarized neutron reflectometry were used to characterize the surface coverages.

The study related the kinetic friction coefficient as a function of shear rate in the hydrodynamic (high shear rate) lubrication regime. A correlation was found to exist between the lubricant penetration and layering with friction coefficient. The effects of the saturation and unsaturation structures for the aliphatic groups were compared depending to the surface coverage. At high surface coverage for both SA and OA films, the results showed very similar properties. At low and intermediate surface coverages, the results showed that the double bond in OA leads to less penetration of lubricant into the surfactant film and less layering of the lubricant near to the film. Furthermore, the results showed that for OA, the friction coefficient had a weak dependence on surface coverage, while the friction coefficient for SA had a strong dependence on surface coverage. The friction coefficient for SA also increased with decreasing surface coverage and allowed more lubricant penetration.

The previous studies concluded that unsaturation bonds in the OA molecule determined the orientation and position of the molecule on the surface. The main effect was to make the OA molecules adopt slightly more upright conformations than SA molecules at high surface coverage.[37] Density studies of OA showed that the surfactant molecules tilted significantly under shear, while calculations of the end-to-end distance showed that the molecules elongated. Equivalent studies on SA show that the molecules did not elongate.

1.4 Summary

Fatty acids have been used successfully to functionalize silicon oxide like surfaces. Oleic and stearic acid molecules have been absorbed chemically on surfaces of glass, mica, tin, lead, gold, Si wafers. Conflicts exist in the times used to functionalize with acids. No study has reported an optimum functionalization time; all previous work used specific functionalization times without confirming whether the time was sufficient or optimal. Finally, previous work has also provided no specific details on how temperature or acid concentration affect the surface coverage.

Chapter 2. Research Proposal

2.1 Goal, Motivation, and Objectives

As stated in Chapter 1, the goal of this study is to determine the best preparation steps to make hydrophilic silicon oxide-like surfaces hydrophobic in a specific way. Figure 2.1 illustrates the motivation for the study. This work will provide the best approach to functionalize microscopically flat hydrophilic surfaces in order to coat them with nanoparticles that have hydrophobic ligands. The ligands are oleic acid. This thesis work will therefore focus on functionalizing surfaces using solutions of oleic or stearic acid. This work will only investigate methods to functionalize silicon-oxide like surfaces, it will not coat the functionalized surfaces with nanoparticles.

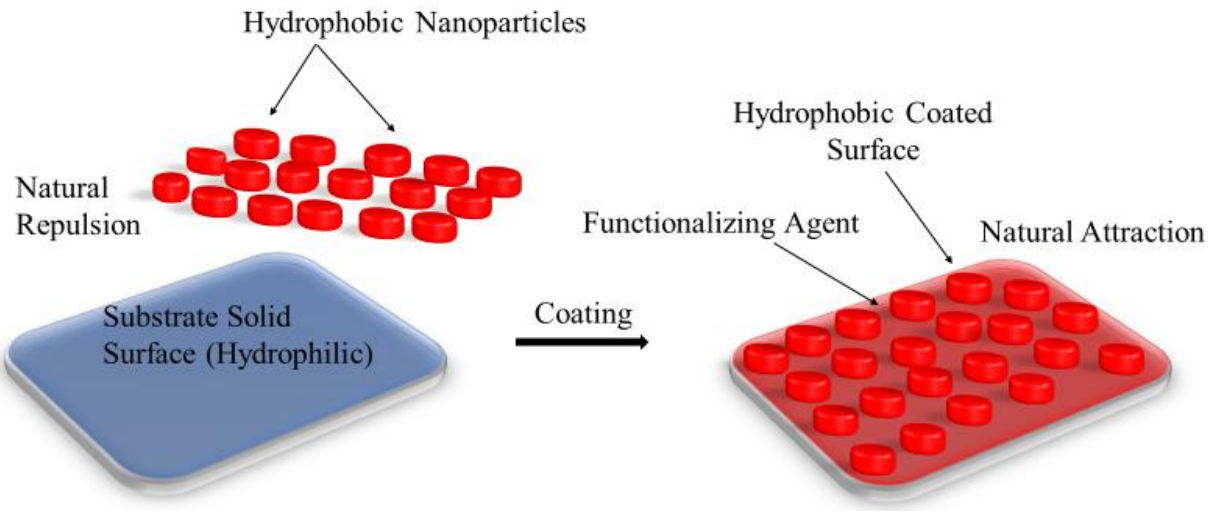

Figure 2.1 Schematic illustration of natural repulsion between a flat hydrophilic surface and hydrophobic nanoparticles. A functionalizing agent changes the hydrophilic surface into a hydrophobic surface to allow the nanoparticles to adhere.

The first objective toward the goal is to define the parameters that could be varied in the study. They include solvents, cleaning methods, temperatures, concentrations, time, and type of silicon oxides-like surface. The second objective is to establish which parameters should be held constant. This work will vary substrate, fatty acids, time, and temperature while holding cleaning methods, solvent, and solution concentration constant. The third objective is to establish the combination of parameters for the study that represent the potential for the most interesting results. The combinations are presented by the hypotheses below. The fourth objective is to carry out the experiment to produce the data. The fifth objective is to analyze and interpret the data collected. The final objective is to validate or invalidate the hypotheses based on the results. We will reach our goal when we meet all of the above objectives.

2.2 Hypotheses

This study has three hypotheses. The first hypothesis is that an optimal reaction time exists to obtain a maximum hydrophobicity for the silicon oxide-like surfaces glass, mica, and Si wafers using wet chemistry deposition of oleic acid at a defined acid concentration C_A (molarity) well enough above a theoretical minimum, Cm (molarity). The theoretical minimum concentration is established in Chapter 3 as the required amount of organic acid in 10 mL solution to coat a 1 cm^2 area of a surface with a perfect monolayer. The acid concentration C_A will be set as a substantial factor above Cm. The optimal reaction time is the limit in time when the degree in hydrophobicity is at maximum and does not increase significantly after a longer functionalization period. This hypothesis implies that overall chemical reaction has a positive order in time, whereby the amount of oleic acid absorbed on the surface increases as time increases. It also limits

the amount of acid that absorbs on the surface in the final state to the surface in the final state to the maximum amount of molecules that can pack together.

The second hypothesis is that the maximum degree of hydrophobicity for silicon oxide-like surfaces is independent of the temperature solutions of oleic acid at the optimal functionalization time and above concentration C_A. This hypothesis implies that the reaction is not a thermodynamic equilibrium reaction. Although the reaction rate may be controlled by temperature, the final amount of reaction is not. In this regard, the reaction is presumed to be an irreversible chemical adsorption process.

The final hypothesis is that silicon oxide-like surfaces that are functionalized with a wet chemistry solution of stearic acid between room temperature to 80 °C, at C_A above Cm, and at the optimal functionalization time have a higher hydrophobicity than the same surfaces functionalized with a wet chemistry solution of oleic acid under the same conditions. This hypothesis arises due to the differences in molecular configurations between stearic acid and oleic acid. Oleic acid has a double bond that restricts free rotation of the aliphatic chain. Stearic acid has no such limitation, and it should therefore be able to pack more tightly on silicon oxide-like surfaces. The more densely packed aliphatic chains in the stearic acid layer will cause a higher hydrophobicity than the less densely packed aliphatic change in the oleic acid.

2.3 Metrics

The validity of the first hypothesis will be tested using a graph of contact angle versus time. The first hypothesis will be true if contact angle plateaus to a maximum value within a certain time. If the contact angle continues to increase even after a

reasonable but limited longer time for an experiment (24 h to 96 h), the surface reaction could be deemed to be too slow to be useful in practice.

The second hypothesis will be tested using a graph of contact angle versus reaction temperature with all other factors staying constant. The hypothesis will be true if contact angle does not vary with solution temperature. If contact angle increases with temperature, the oleic acid molecules may be packing more tightly as temperature increases. If contact angle decreases with temperature, the surface may be less packed with oleic acid molecules.

The third hypothesis will be tested using a graph of contact angle versus reaction temperature. The hypothesis will compare surfaces coated with stearic acid at Cm, at the optimal functionalization time, and at defined increments in temperature compared to surfaces coated with solution of oleic acid under the same conditions. If the maximum hydrophobicity is recorded with surfaces that are coated with stearic acid, the molecules of stearic acid may be packing the surfaces more densely than the molecules of oleic acid.

2.4 Outcomes

Validating the first hypothesis will tell us that the oleic acid wet chemistry deposition does not require infinite time to functionalize silicon oxide-like surfaces. We will also not have to guess the optimal functionalization time. Validating the second hypothesis will tell us that the maximum hydrophobicity of silicon oxides-like surface is independent of solution temperature at optimal functionalization time. Increasing the oleic acid solution temperature will not increase the maximum hydrophobicity at the functionalization time. Finally, by validating the third hypothesis, we will know how the structure of fatty acids plays a key role in determining the degree of hydrophobicity.

Specifically, an aliphatic fatty acid with double bonds will be less favorable to make the surface hydrophobic.

2.5 Significance and Impacts

Fatty acids are less expensive per unit amounts than silanes to obtain the same degree of hydrophobicity. Fatty acids are cheaper and more biocompatible than silanes. The chemistry of silanes can be tweaked to still have the same degree of hydrophobicity while the degree of hydrophobicity of acids is not stable.

Across literature,[43,44,47] no clear methodology has been given to establish a reproducible methodology to coat with fatty acids that can be used in variation across temperature, concentration, time and solvents. The significant impact is to establish a recipe that can be used across systems.

Chapter 3. Experimental Approach

3.1 Materials and Supplies

Glass substrates were Premium cover glass slips (regular glass) type No.12-548-A, lot # 032315-9, with dimensions of 18 mm x 18 mm x 1mm from Fisher Scientific. Silicon substrates were cut from Prime grade wafers, the 100 mm p-type boron doped 1-100 ohm-cm, 4", SSP 500,100 mm P (100) ohm-cm SSP 500 um from Sigma Aldrich. Mica samples were cut from 6.5 cm x 2.5 cm mica substrates from an unknown vendor. Oleic acid grade at 99.5% was from Fisher Scientific. Stearic acid was grade at 97% from Sigma Aldrich. The solvent ethyl alcohol (200 % proof), the cleaning chemicals methanol (MeOH, 98%), the hydrochloric acid (HCl, 38.0 %), and the concentrated sulfuric acid (H_2SO_4, 96 %) were from Fisher Scientific. Deionized (dI) water was obtained from an Evoqua Water Technologies Inc. deionizing unit in the chemistry department.

Plastic test tubes at 15 mL and 30 mL with reference number Falcon REF 352096 were from Fisher Scientific. Thirty (30 mL) glass test tubes were from Fisher. The hot bath was a Thermo Scientific Precision GP 10 from Fisher Scientific. Samples were stored in a Bel Art SP Scienceware cabinet desiccator from Grainger. Samples were processed in plastic wells culture plates with flat bottom from Corning Incorporated. Solution were processed using sterile 10 mL syringes DG 565001 from LUER-LOK ^{TM} Beckton Dicksinson & Co. and Pyrex glass petri dishes of 35 mm from Fisher Scientific. Scotch tape was from 3M.

3.2. Surface Cleaning

3.2.1 Glass

Figure 3.1 below gives an illustration of the glass cleaning process. For each experiment, six (6) glass coverslips were cleaned using a glass cleaning protocol from the literature.[48] The protocol reported a 1:1 solution of methanol (MeOH) and hydrochloric acid (HCl). A solution of 100 mL of MeOH and 100 mL HCl was mixed in 250 mL baker. A 12 wells culture plate was used to allow the glass substrates to stand vertically. Vertical immersion of the samples allowed both sides of the glass substrates to be in contact with the solution. The immersion time was 30 min. After the glass samples were taken out, they were rinsed with dI water and immersed for 30min in a solution of H_2SO_4 using another 12 wells culture plate with flat bottom to allow the glass substrates to stand vertically. The glass samples were then rinsed with dI water and submerged in an ethyl alcohol bath for 30 min to further remove any possible contaminants.[49]

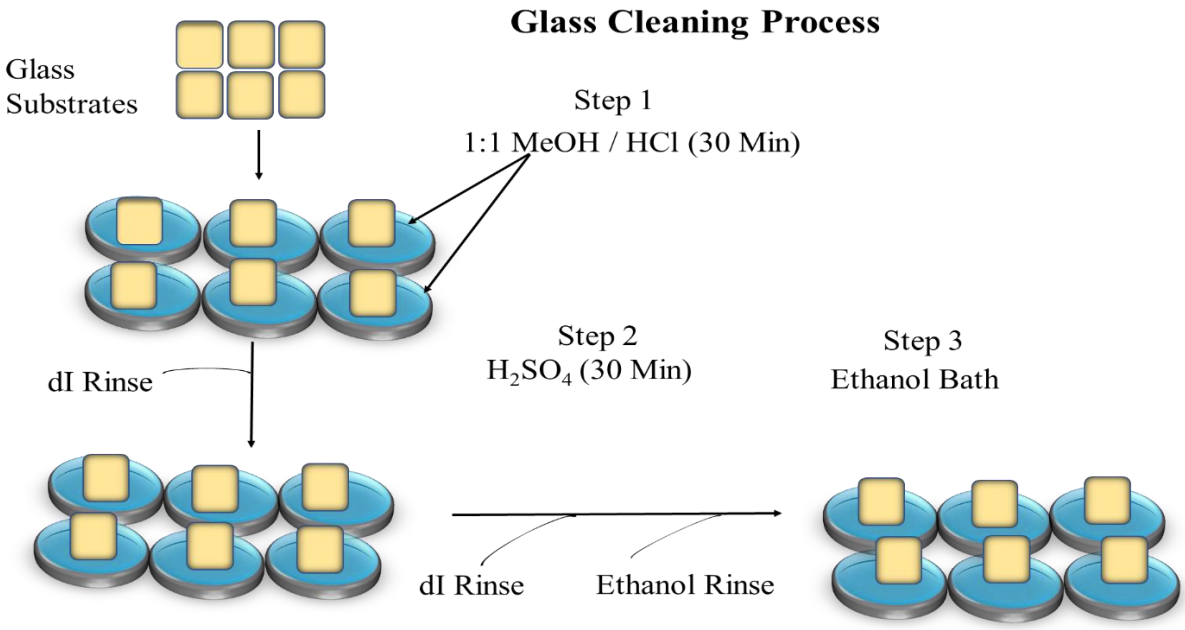

Figure 3.1 Schematic illustration of the glass cleaning process. In step 1, the glass substrates were immersed for 30 min in a 1:1 MeOH / HCl solution. In step 2, they were rinsed with dI water and immersed in H_2SO_4 for 30 min. In step 3, the substrates were rinsed with dI water and then with ethanol before they were submerged for 30 min in an ethanol bath.

3.2.2 Si Wafers

Figure 3.2 on the next page gives schematic illustration and description cleaning processes for Si wafers. Six (6) experiments each were carried out for each functionalization time. Each repeat experiment went through the same cleaning procedure. The Si substrates were cut into pieces of dimension 1 cm x 2 cm each. The samples were cleaned using a wet chemistry method referred to as standard cleaning method from the literature.[50] The cleaning method uses solutions called standard cleaning 1 (SC1) and standard cleaning 2 (SC2). The SC1 solution was made of 5:1:1 ratio of dI water to hydrogen peroxide (H_2O_2) to ammonium hydroxide (NH_4OH). The SC2 solution was a 6:1:1 ratio of deionized water to H_2O_2 to HCl. The SC1 and SC2 cleaning were processed in glass petri dishes and heated to a temperature of 80 °C on a hot plate before the cleaning began. The Si wafers were immersed in the SC1 on the hot plate for 15 min, rinsed with deionized water, immersed in the SC2 at 80 °C on the hot plate for 15 min, and rinsed again with dI water at room temperature. The clean samples were put in an ethanol bath and taken out after 30 min immediately when ready to be functionalized.

3.2.3 Mica

The mica samples were cleaned with a tape method. In this method, a piece of tape is attached over the strip of mica, pressed firmly in place, and then lifted from the mica. This removes a layer of the surface as a cleavage plane. After the samples were cleaved with tape, they were rinsed with ethanol, and left in an ethanol bath for 30 min before functionalization.

3.3 Surface Functionalization

3.3.1 Theoretical Minimum Concentration

The theoretical minimum concentration Cm (mols / L) is defined as the concentration of fatty acid needed in 10 mL solution to have exactly enough molecules to cover a 1 cm x 1 cm

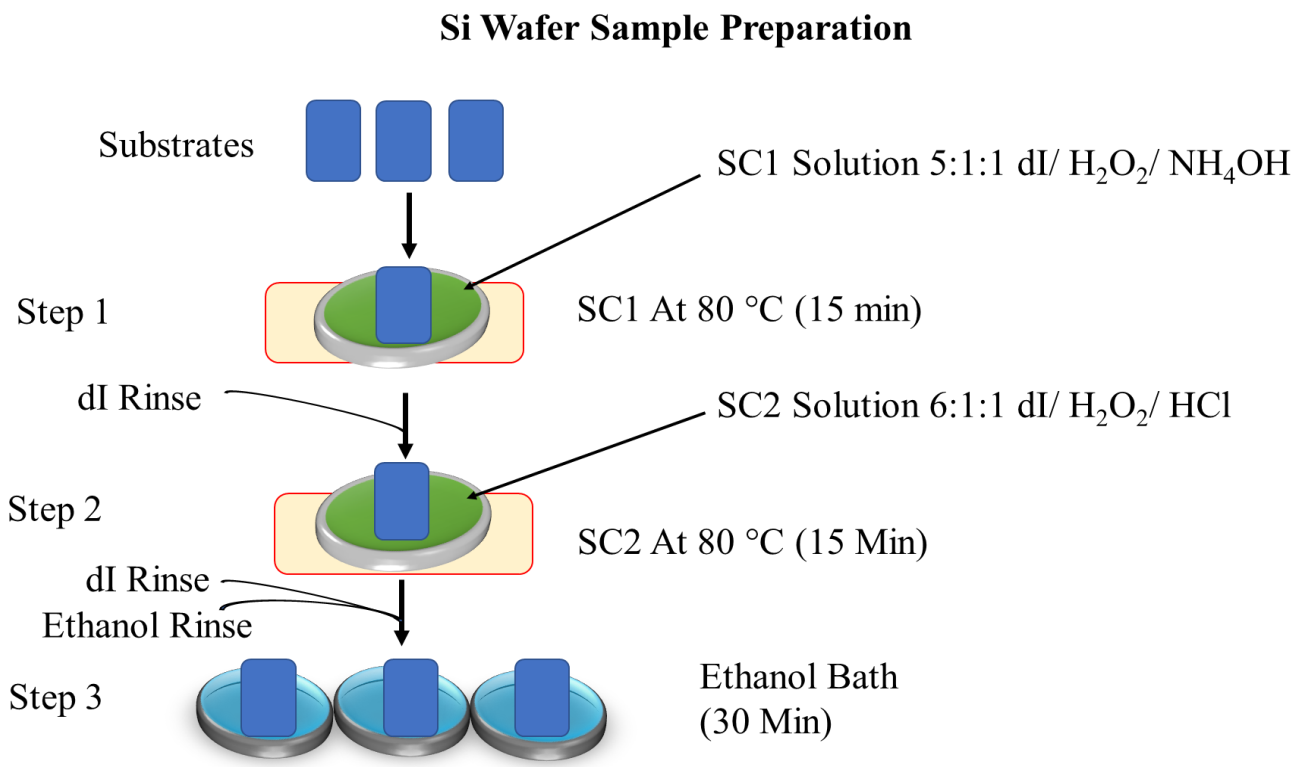

Figure 3.2 Schematic illustration of the set up to process Si wafers. In Step 1, the Si substrates were immersed in a SC1 solution (a 5:1:1 solution of dI / H_2O / NH_4OH) on a hot plate for 15 min then rinsed with dI water. In Step 2, the substrates were immersed in a SC2 (a 6:1:1 solution of dI / H_2O / HCl) at 80 °C on a hot plate for 15 min rinsed again with dI water at room temperature. In step 3, the clean samples were rinsed with ethanol before they were left in an ethanol bath for 30 min.

substrate with a perfect single monolayer. The reason that Cm is determined is to know the solution concentration limit to have just enough acid molecules to coat the surface. The solution concentration for the study was subsequently set at least 100 times Cm so that the maximum change in the concentration will be below 1% at an expected coverage of one monolayer of close packed OA molecules.

The adsorption and positional mechanisms of the fatty acid molecule on the surface of the substrate play a key role in Cm determination. A fatty acid molecule is made up of a R group, the acid hydrophobic tail, and a carboxyl COOH. Literature reports that the carbon atom of the carboxylic group of a fatty acid has an sp^2 configuration and the atoms have bond angle of 120°. The acid molecule anchors to the surface of a silicon oxide-like surface through the esterification

reaction.[20,27,44,47] The carboxyl group is the reactive site. The carboxyl group on the acid attaches to the atom of the silicon on the surface.

Figure 3.3 below gives schematic illustration of a carboxyl group atom to one possible configuration to attach to a silicon-oxides like substrate surface. The bonds between the oxygen atom of the carboxylic group of the acid and the silicon atom of the surface (Si-O) bonds to form a tetrahedron, and the R group extends outward from the surface given the surface its hydrophobicity. The radius of the carbonyl C=O ($l_{C=O}$) (m), the length of the carbon-oxygen (l_{C-O}) (m), the length of the carbon -carbon (l_{C-C}) (m) were all factored into the calculation of the exclusion radius r_m (m) along the surface.

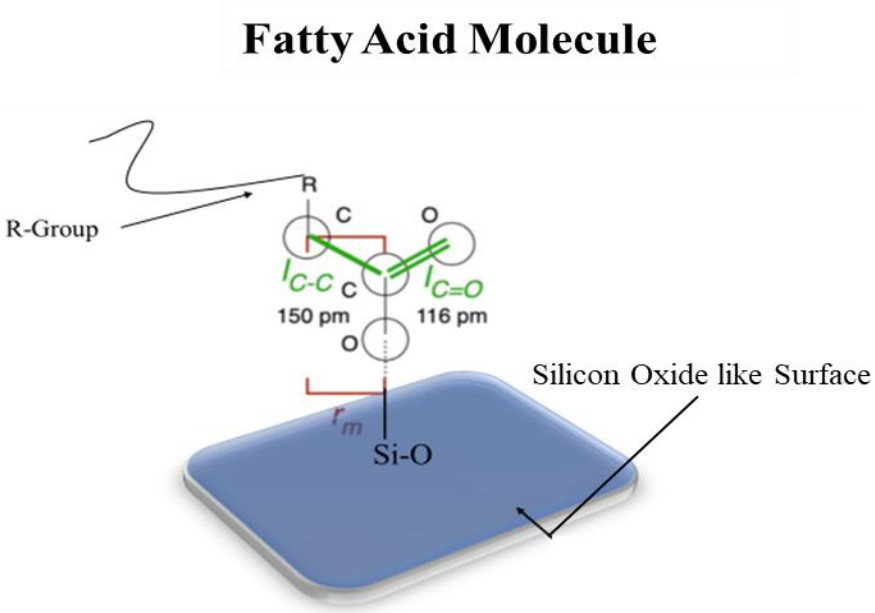

Figure 3.3 Schematic illustration of a fatty acid molecule attached to a silicon oxide-like substrate surface. The fatty acid molecules attach to the surface via the carboxyl group. The hydrophobic R-group is not directly involved into the attachment process. The silicon atom of the surface bonds 90° with the oxygen atom of the carboxyl group and forms a tetrahedron.

Figure 3.4 gives a schematic illustration of the view looking down on the surface at the absorbed molecule. The exclusion radius r_m is the circle that is swept out by the molecule

rotating on the surface. The radius prohibits the acid molecules from contacting each other as they are packing the substrate surface.

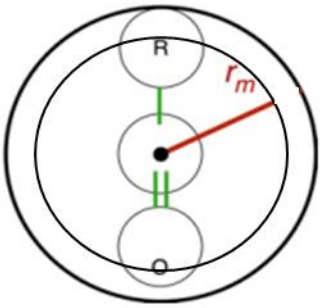

Figure 3.4 Schematic illustration of the view looking down of the absorbed molecule of the fatty acid on the silicon-oxide like substrate surface. The exclusion radius r_m is shown in red and the carbon atom is in the center of the circle.

The closest lateral packing of molecules forms a rhombohedron as shown in Figure 3.5. When the acids molecules pack in this hexagonal packing, one molecule occupies each rhombohedron. The hexagonal packing allows the molecule to pack tightly and form a monolayer on the surface of the substrate.

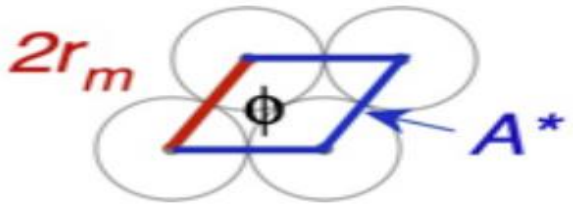

Figure 3.5 Schematic top view of hexagonal packing of fatty acid molecules on the silicon-oxide like surface. Each circle exclusion radius contains one molecule anchoring the surface.

Given values for the radius of the carbonyl[51] and the length of the Si-O bond[52] were used to determine the theoretical minimum concentration. The exclusion radius r_m of the attached OA molecule is define from geometry as

$$r_m = l_{cc} \sin(60°).$$

The area of the rhombus in hexagonal packing of molecules is

$$A = 4r^2_m \sin(60°).$$

The rhombus unit cell contains one OA molecule in close packing. The number density of molecules per unit area is therefore $\rho NoA = 1/A$ (molecules). The number of molecules to cover 1 cm^2 area is

$$N_1 = \rho NoA = 1/A.$$

The minimum concentration Cm (mols/L) is formed from this many molecules in 10 mL solution

$$Cm = (N1/No)(1/0.01),$$

where M_{OA} is molar mass (g/mol) and No is Avogadro's number (molec/mol). Reference and calculated values are reported in Table 3.1 below.

Table 3.1 Reference values used for the calculations of minimum solution concentration of oleic acid.

Value		Reference
l_{c-c}	150 pm	51,52
r_m	$1.3\ 10^{-8}$ cm	calculated
A	$5.85\ 10^{-16}\ cm^2$	
M_{OA}	282.46 g/mol	51
$\rho N,OA$	$1.71\ 10^{15}$ molec /cm^2	
Cm	0.28 μM	

The minimum theoretical concentration to cover 1 cm^2 surface with a perfect monolayer of OA from 10 mL solution is 0.28 μM. The value Cm is an experimental design factor while the surface area of the substrate and the solution volume are the controlling factors in setting the solution concentration. If the surface area is multiplied by factor F at the same solution volume, the solution concentration must increase by a factor F. By example, when functionalizing

10 cm^2 area, the concentration in 10 mL solvent must be 10 times higher. Alternatively, if the solution volume is increased by factor F with the same surface area, the solution concentration must be cut by the same factor F. By example, when the given values of a substrate of 1 cm^2 of surface area sample in 20 mL of solution, the theoretical minimum concentration is 0.14 μM. Also, Cm is for tightly packed molecules in a monolayer configuration. If the acid molecules on the surface have higher exclusion radius than shown in Figure 3.3, the calculated theoretical minimum concentration will be lower. Based on the algebraic formulations, doubling the exclusion radius would cut the theoretical minimum concentration by a factor of four.

The given substrate surface was approximately 4 cm^2 surface area. In 10 mL solution, the theoretical minimum concentration, Cm is 1.12 μM. In the work that follows below, all substrates were functionalized with a nominal concentration CA of at least 100 times Cm. For the majority of samples in this work, this concentration was used for all experiments, especially since the glass area did not equal the Si wafer area. The value of Cm was taken to be independent of the choice oleic or stearic acid.

3.3.2 Glass Functionalization

For functionalization at room temperature, six (6) glass coverslips with total area of 3.8 cm^2 were functionalized in 10 mL solution at 0.112 mM OA in ethyl alcohol solution. This concentration was at least 120 times above theoretical minimum concentration. Plastic tubes of 30 mL were used for room temperature functionalization. The shape of the plastic tubes allowed the glass substrates to remain vertical while reacting. Figure 3.6 on the next page shows an example of the set up. Samples were immersed for 3 min, 10 min, 30 min, 100 min, 300 min, 600 min, 1,000 min, 1,200 min, and 3,600 min at room temperature. The glass samples had been left sitting in ethyl alcohol bath for 30 min prior to any oleic acid functionalization. One clean

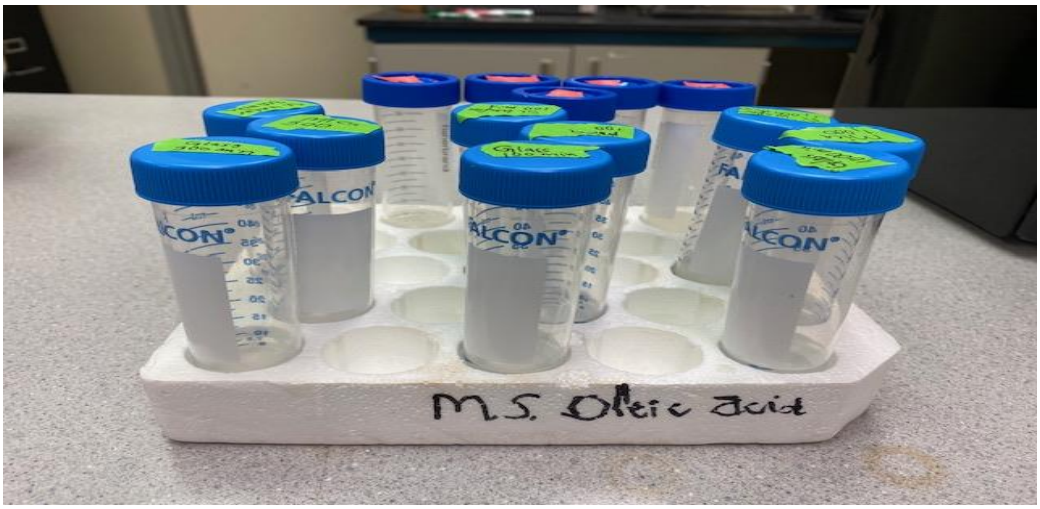

Figure 3.6 Plastic test tubes were used to immerse glass, Si wafers, and mica substrates in solutions of OA at room temperature for various functionalization times.

glass was dried over night at 150 °C to be used as standard. After being functionalized, the glass samples were dried overnight at 150 °C and stored in an air sealed desiccator for no longer than an hour before analysis. The experiment was repeated with six (6) repeat experiments carried out at each functionalization time for glass substrates at room temperature.

Analysis of the 6 repeat experiments at room temperature found that 1,000 min appeared to be an optimum functionalization time. Correspondingly, six glass samples were functionalized with oleic acid at 1,000 min using a hot bath unit as shown in Figure 3.7. Temperatures were set in separate experiments at 50 °C, 60 °C, 70 °C, and 80 °C. The glass test tubes still allowed the substrates to remain vertical. After being dried overnight at 150 °C, the samples were stored in an air sealed desiccator cabinet for no longer than one hour before characterization.

A 0.112 mM solution of stearic acid in ethyl alcohol (the solution was 120 times Cm) was used to functionalize glass substrates at 1,000 min as functionalization time in separate experiments room temperature, 50 °C, 60 °C, 70 °C, and 80 °C. The samples were submerged vertically in glass test tubes. Rubber corks were used to seal to the top of the test tubes, and 10 mL syringe needles were inserted in the rubber corks to let out the pressure built from the

Figure 3.7 Hot bath for glass functionalization. A metal basket was used to hold glass test tubes in place while they are immersed in the hot water bath.

mixture being heated. The functionalized samples were dried overnight at 150 °C and stored in an air sealed desiccator for no longer than one hour before they were characterized.

3.3.3 Si Wafer Functionalization

Six (6) substrates of Si wafers were functionalized in a mixture of 0.112 mM oleic acid in ethyl alcohol (150 times Cm) in separate experiments for 3 min, 10 min, 30 min, 100 min, 300 min, 600 min, 1,000 min, 1,200 min, and 3,600 min at room temperature. Plastic tubes of 30 mL were used for room temperature functionalization. The substrates remained vertical while they were being functionalized. One clean Si wafer sample was dried over night at 150 °C to be used as standard. After the functionalization, each Si wafer sample was dried overnight at 150 °C and stored in an air sealed desiccator for no longer than one hour before analysis. The process was repeated with 6 experiments carried out at each functionalization time for Si wafer substrates at room temperature.

After the sample analysis, a trend similar to glass functionalization was observed. The maximum optimum functionalization time appeared to be 1,000 min. Six (6) Si wafer samples were functionalized at 1,000 min with oleic acid using a hot bath unit at 50 °C, 60 °C, 70 °C, and 80 °C for 1,000 min. The same hot water bath setup used for glass substrates was used for the Si wafers temperature variations (Figure 3.6). The Si wafer samples were dried overnight at 150 °C and stored in an air sealed desiccator cabinet before being characterized.

A 0.112 mM solution of stearic acid in ethyl alcohol (150 times Cm) was used to functionalize Si wafers substrates at 1000 min and at room temperature, 50 °C, 60 °C, 70 °C, and 80 °C. The samples were submerged vertically in glass test tubes. Rubber corks were used to seal to the top of the test tubes, and 10 mL syringe needles were inserted in the rubber crocks to let out the pressure built from the mixture heating. After being functionalized for 1,000 min, the samples were dried overnight at 150 °C and stored in an air sealed desiccator for no more than one hour before they were characterized.

3.3.4 Mica functionalization

Mica substrates were functionalized in the same process as in the functionalization of glass, and Si wafers. The room temperature as well as the hot bath set ups were similar to the ones used on glass and Si wafers substrates. a mixture of 0.112 mM oleic acid in ethyl alcohol (150 times Cm). Samples of 1cm x 2 cm were functionalized at 3 min, 10 min, 30 min, 100 min, 300 min, 600 min, 1,000 min, 1,200 min, and 3,600 min. The samples were dried overnight at 150 °C and kept in an air sealed desiccator for no more than one hour prior to characterization.

A 0.112 mM solution of stearic acid in ethyl alcohol (150 times Cm) was used to functionalize mica for 1000 min at room temperature, 50 °C, 60 °C, 70 °C, and 80 °C. The samples were submerged vertically in glass test tubes in the same process as glass and Si wafers.

After being functionalized, the mica samples were dried overnight at 150 °C and stored in an air sealed desiccator for no more than one hour before they were characterized.

3.4 Characterization and Data Analysis

A Ramé-Hart model 290 F4 goniometer shown in Figure 3.8 was used to obtain contact angles of samples. Hardware components are defined in the figure. The system included version 2.0 of DropImage software.

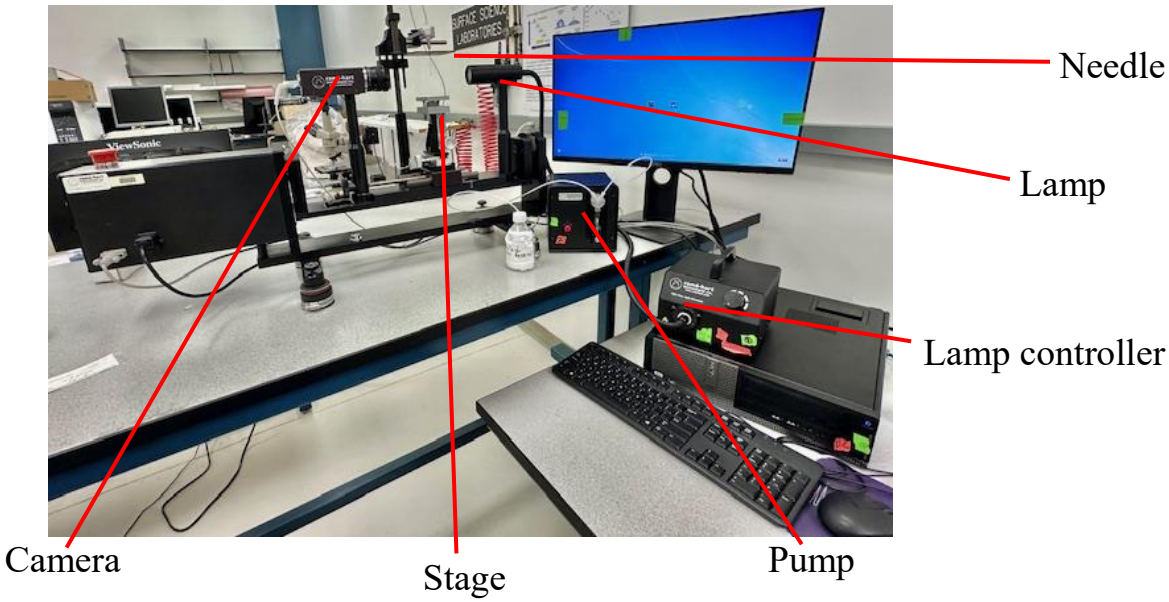

Figure 3.8 Ramé-Hart model 290 F4 goniometer system. The system is composed of a pump, a lamp and controller, a camera, a stage platform for samples, a screen monitor, and a computer. Drops were deposited using a syringe needle at 0.5 mm diameter.

Contact angles of water were measured using 4.0 μL droplets at three different positions per sample. Five contact angle measurements were taken per position at an interval of 0.2 s. The left and right contact angles were recorded for each drop. Each data point in all graphs of results contact angle represents the average and standard uncertainty from 2 sides (left and right) x 5 measurements over time per drop x 3 drops per sample x 6 samples per experiment. This is equivalent to doing 18 repeat experiments to vary the location on a sample surface with the same chemistry.

Chapter 4. Results and Discussion

4.1 Experiments on Mica

Functionalization on mica gave inconsistent results. On some surfaces, contact angles were significantly different on the left and right sides of the drop. The values could not be repeated at different locations on the same sample and on different samples. With visual inspection, the OA also appeared to change the structure of the mica surface microscopically. The observations are consistent with a proposal that the oleic acid solution etches through or between the cleavage planes of the mica to remove or lift them during the wet chemistry process. In this respect, vapor deposition, as noted elsewhere[53] would be preferred for mica. The results on mica are considered unreliable to report. The discussions below therefore only focus on results from functionalizing glass and Si wafers.

4.2 Hypothesis One

Figure 4.1 on the next page shows representative images for the contact angle drop on a clean glass substrate (1a) and on a glass substrate at its highest contact angle (1b). On the clean glass substrate, the droplet is indicating hydrophilic nature with contact angle of 37° for the left side and 38° for the right side. On the functionalized glass substrate, the droplet is indicating a hydrophobic behavior with a contact angle of 109° for the left side and 108° the right side. On

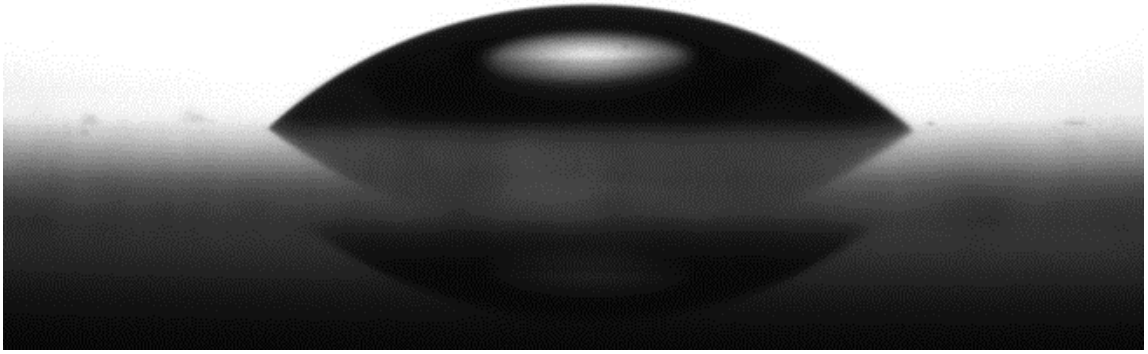

(1a)

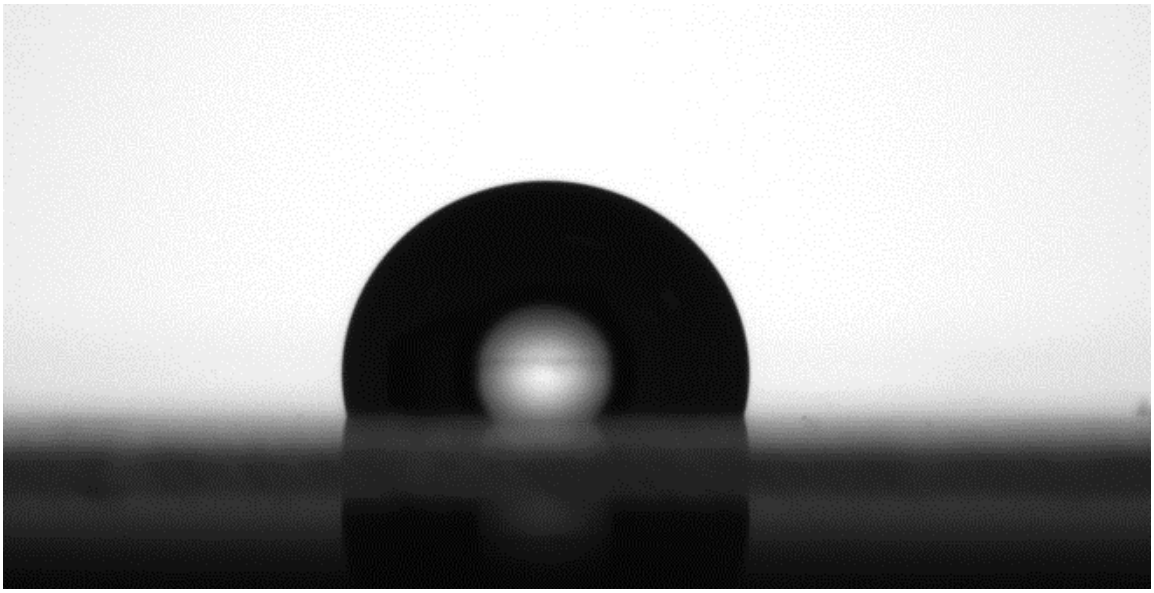

(1b)

Figure 4.1 Representative contact angle image for clean glass (4.1a) and for glass at highest contact angle (4.1b). On clean glass, the droplet is indicating hydrophilic nature with contact angle of 37° for the left side and 38° for the right side of the droplet. On the functionalized glass, the droplet is indicating a hydrophobic behavior with contact angle of 109° for the left side and 108° for the right side.

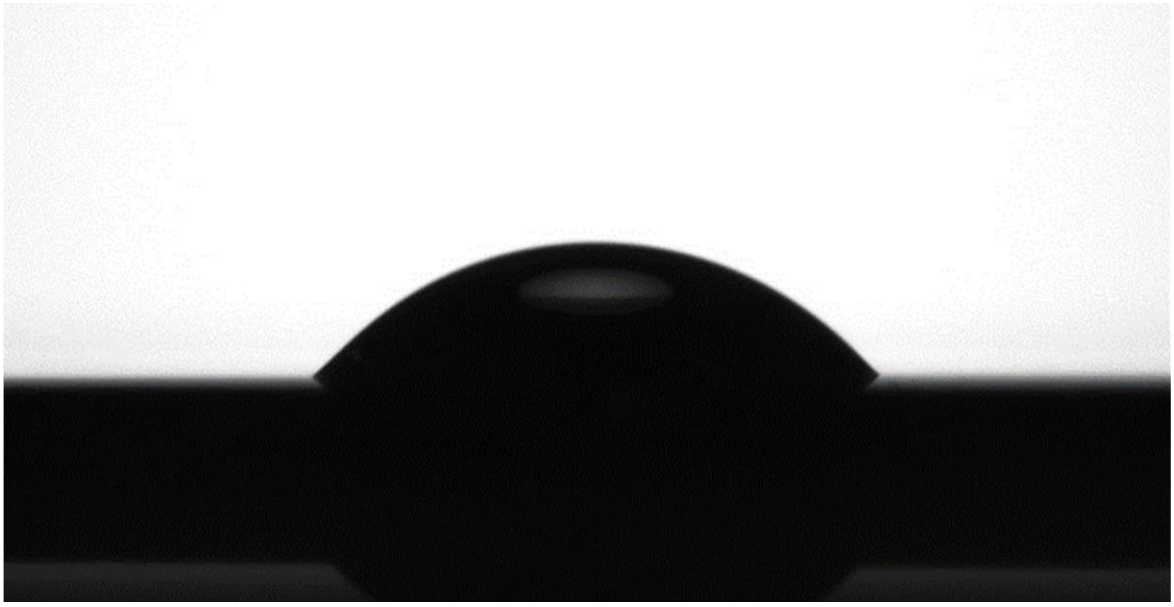

(2a)

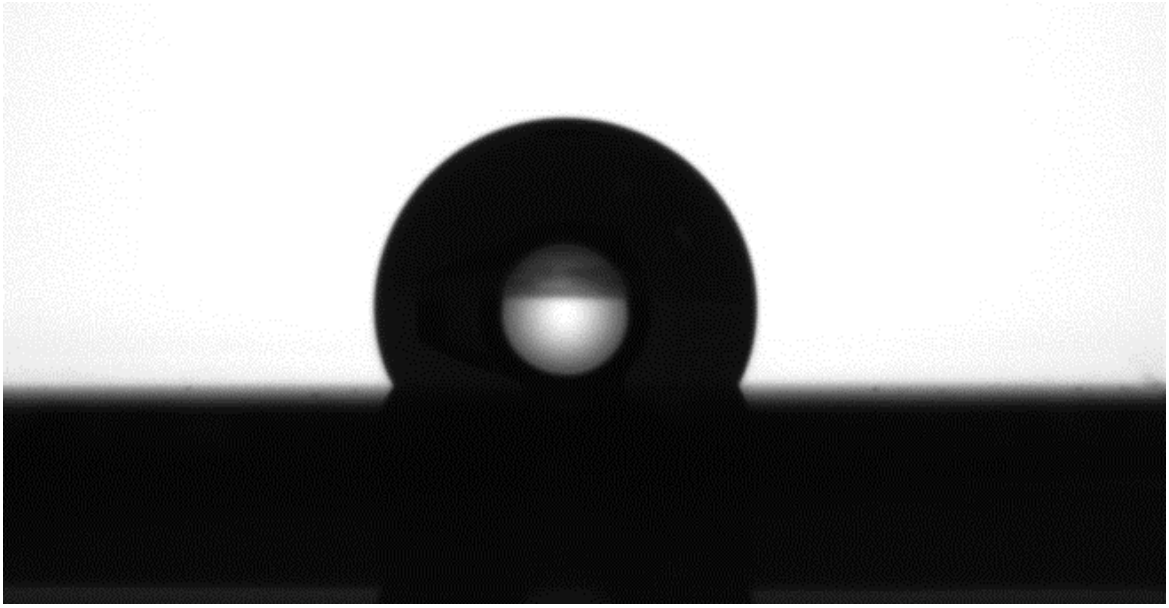

(2b)

Figure 4.2 Representative contact angle image for clean Si wafer (4.2a) and for Si wafer at highest contact angle (4.2b). On the clean Si wafer, the droplet is indicating hydrophilic nature with contact angle of 37° for the left side and 38° for the right side of the droplet. On the functionalized Si wafer, the droplet is indicating a hydrophobic behavior with contact angle of 116° for the left side and 114° for the right side.

right side. On the functionalized Si wafer, the droplet indicates a hydrophobic behavior with contact angles of 116° on the left side and 114° on the right side.

Figure 4.3 on the next page shows contact angles for OA on glass measured as a function of functionalization time. The data points represent averages and standard uncertainties from 18 measurements at each time. Clean glass has a contact angle of 39° ± 2°. As functionalization time increases, contact angle remains constant at about 50° until approximately 300 min. Contact angle then increases, reaching maximum value of 108° ± 4° at 1,000 min. Contact angle decreases after 1,000 min. By 3,600 min, the contact angle is 63° ± 5°.

Figure 4.4 on the second next page shows contact angles for OA on Si wafers measured as a function of functionalization time. The data points represent averages and standard uncertainties from 18 measurements for each time. Clean Si wafers has a contact angle of 38° ± 1°. As functionalization time increases, contact angle remains constant at about 50° until approximately 300 min. Contact angle increases reaching maximum of 115° ± 5°at 1,000 min. Contact angle decreases after 1,000 min. By 3,600 min, the contact angle is 60° ± 5°.

Hypothesis one stated that an optimal reaction time exists to obtain a maximum hydrophobicity for silicon oxide-like surfaces using wet chemistry deposition of OA at a concentration well enough above the theoretical minimum. Respectively, Figures 4.3 and 4.4 indicates that for glass and Si wafers a maximum does exist. In both cases, the maximum occurs at 1,000 min functionalization time. The maximum contact angle is 108° ± 4° for glass and 115° ± 5° for Si wafers. The two values overlap at their bounds of uncertainties and therefore are not considered to be different from each other. Hypothesis one appears to be valid. The type of silicon oxide-like surface appears to have no effect on the optimal time to functionalize. Both Si wafers and glass coverslips had a maximum hydrophobicity at 1,000 min.

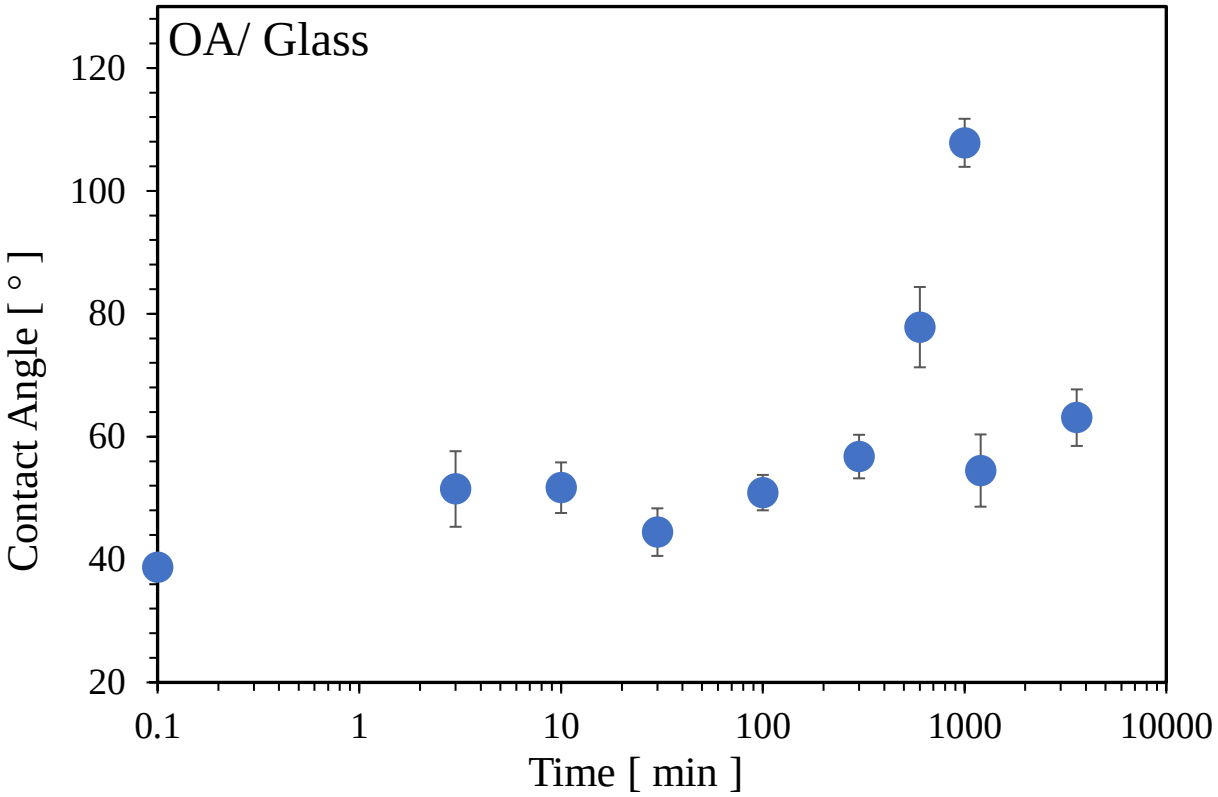

Figure 4.3 Results for the contact angle of OA on glass as a function of functionalization time. Each data point represents 18 measurements. The clean value at 0.1 min is 39° ± 2°. Over time, the values remain constant until approximately 600 min. The maximum value at 1,200 min is 108° ± 4°. The values decrease after 1,200 min to a final value around 63°± 5°.

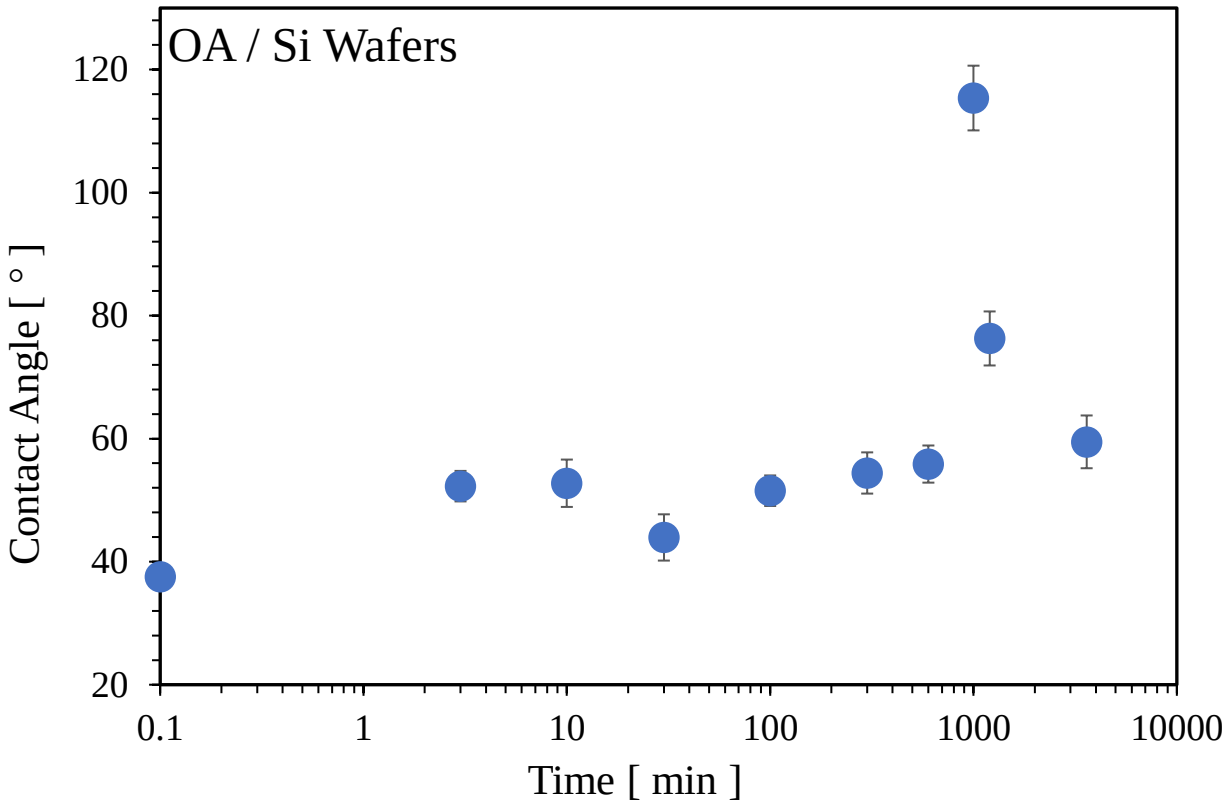

Figure 4.4 Results for the contact angle of OA on Si wafers as a function of functionalization time. Each data point represents 18 measurements. The clean value at 0.1 min is 38° ± 1°. Over time, the values remain constant until approximately 600 min. The maximum value at 1,200 min is 115° ± 5°. The values decrease after 1,200 min to a value around 60°± 5°.

Literature studies have reported functionalization times with no reference to whether they were optimum times. One work reported using a functionalization time at 20 h for OA and SA in n-decane on mica,[43]another reported using a functionalization time at 24 h for OA in ethyl alcohol on three type of glass that included soda-lime-silicate glass, silica slide glass, and soda-silicate glass,[20] and another reported using a functionalization time at 4 h for OA in n-hexane on silicon oxide nanoparticles.[20] In reference to the previous reports, the study at 4 h may not have used sufficient time to obtain an optimal coverage of acid on the surface. This work results are for the optimum functionalization time of organic acid at 1,000 min or 17 h.

The composition of a silicon dioxide surface has been shown to play a role in the interaction of OA on different types of glass.[44] Metal ions can alter the surface charge, resulting in pH changes in the solution of the acid that may change in the dissociation of hydroxyl groups.[34] Metal ions are not expected for either silicon oxide surface used in this work. No significant differences were therefore expected for the glass or Si wafer substrate in optimal time or amount of hydrophobicity, and none were observed.

When an OA molecule absorbs on a silicon-oxides like surface, the absorption is reported to happen at the carboxyl group to form a carboxylate, and the carboxylate forms a chemical adsorption monolayer.[47] The structure of the monolayer was found to be influenced by the concentration of the OA. After the acid molecules saturated the surface in a monolayer, the packing was proposed to change to a bilayer. The bilayer was proposed to consist of inverted stacking of acid on the surface. The chemical - physical bilayer was instable in nature. As time elapsed, the bilayer would collapse and reform itself.

Figure 4.5 on the next page gives schematic representations of the acid in a monolayer and in the proposed chemical – physical bilayer. In the left most figure, the aliphatic group tails

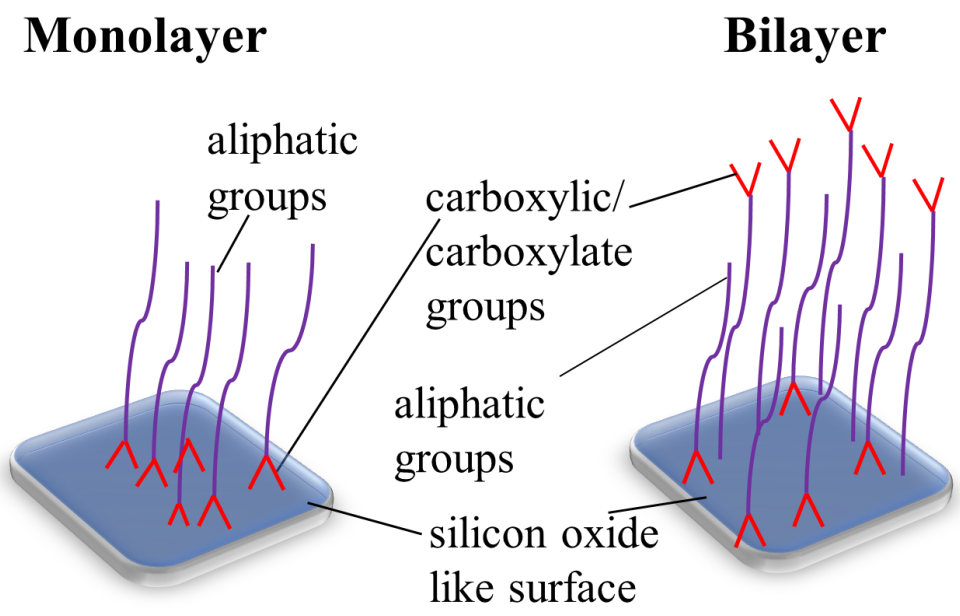

Figure 4.5 Schematic representation of an acid monolayer formation on the left and an acid bilayer on the right. The bilayer is proposed to form after for long immersion times due to high concentrations of excess acid in solution.

of the acids are responsible of making the surface hydrophobic. At lower concentration where the bilayers do not form, the acid molecules have the aliphatic groups exposed on the surface, giving it the hydrophobicity. As the concentration increases, the acid molecules invert and stack up on top of each other, forming the bilayer. The carboxylic groups trap the aliphatic groups. The trapping of the aliphatic groups by the carboxylic groups makes the surface hydrophilic.

The results in contact angle Figure 4.3 and Figure 4.4 are consistent with the formation and break up of a chemical – physical bilayer. Starting from the initial time, the OA absorbs on the surface and forms a monolayer. The contact angle increases because the aliphatic tails of the OA are exposed outward from the surface. As time progresses the bilayer reforms with the hydrophilic carboxylic groups trapping the aliphatic groups rendering the surface hydrophilic.

The experiments for Figures 4.3 and 4.4 used a concentration of OA at or above 100 Cm. At this concentration, the surface can become saturated with a monolayer of OA molecules. The

excess OA molecules from the solution will then be driven by thermodynamics to form a surface multilayer. The inner molecules are bound to the surface chemically, and the outer molecules are intertwined through van der Waals forces. This explanation, if true, recommends that future studies should be done at significantly lower concentrations for OA in solution to avoid the possibility of forming a surface bilayer.

The abrupt decrease of the contact angle after 1,000 min could also be attributed to chemical reaction between the silicon oxides like surface and the fatty acids. After the acids functionalize the surface, they may etch it rendering it hydrophilic again. This option is considered less likely than forming a bilayer.

4.3 Hypothesis Two

Hypothesis two stated that the maximum degree of hydrophobicity for silicon oxide-like surfaces is independent of the temperature solutions of OA at the optimal functionalization time and above concentration Cm. The hypothesis was investigated using studies that varied solution temperature with all else constant. Figure 4.6 on the next page shows results for contact angles of OA on glass measured as a function of temperature. The data points represent average and standard uncertainties from 18 measurements. Starting at room temperature with a contact angle of 108 ± 4°, the value drops to 87° ± 4° at 50 °C. The value starts increasing again until reaches 101° ± 3° at 80 °C. Figure 4.7 shows results for contact angles of OA on Si wafers. At room temperature with the contact angle is 115° ± 5°. The value drops to 92° ± 4° at 50 °C. The value remains constant at 60 °C. The value starts increasing until it reaches 116° ± 6° at 80 °C.

Hypothesis two proposed that the maximum degree of hydrophobicity for silicon oxide-like surfaces is independent of the temperature solutions of OA at the optimal functionalization time and above concentration Cm. Both Figures 4.6 and 4.7 respectively for OA on glass and OA

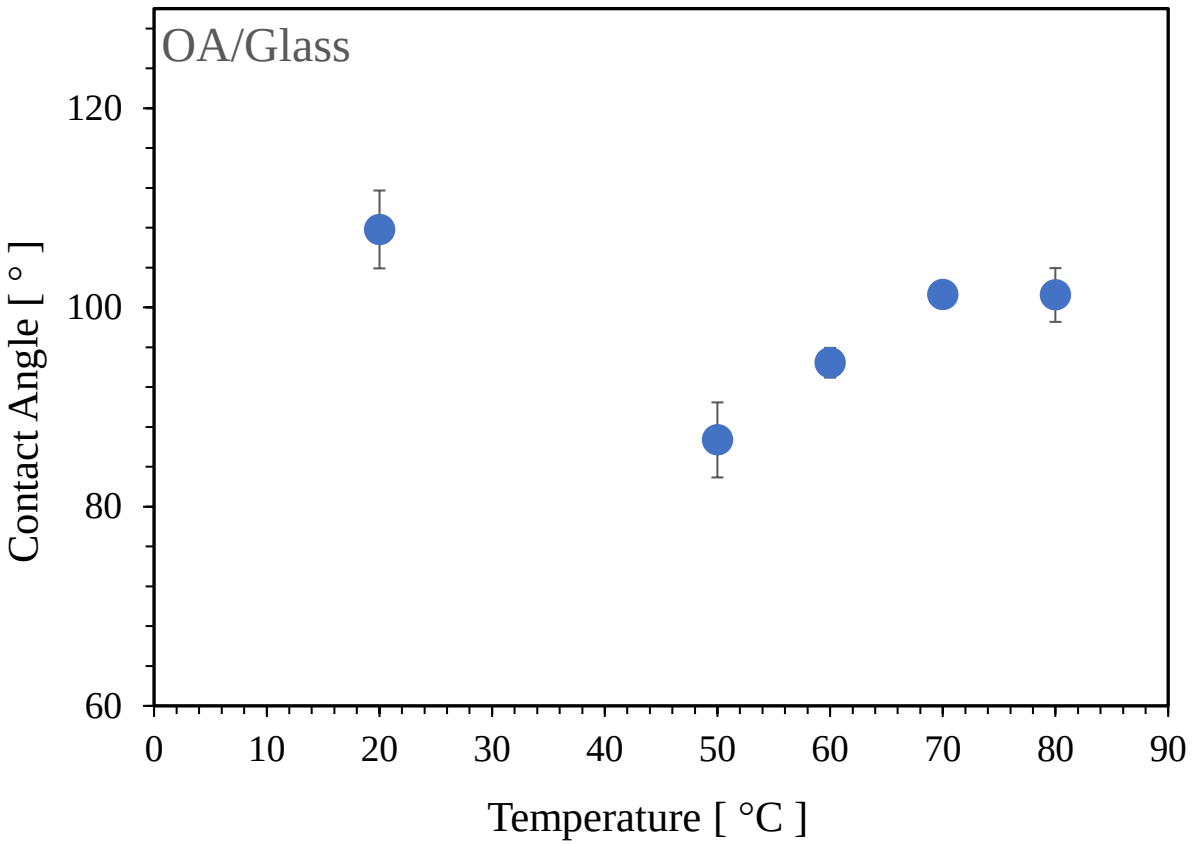

Figure 4.6 Results for contact angles of OA on glass as a function of temperature. The data points represent 18 measurements. At room temperature contact angle value is 108° ± 4°. The value drops to 87°± 4° at 50 °C as the temperature increases. The value increases to 101° ± 3° at 70 °C and remains constant.

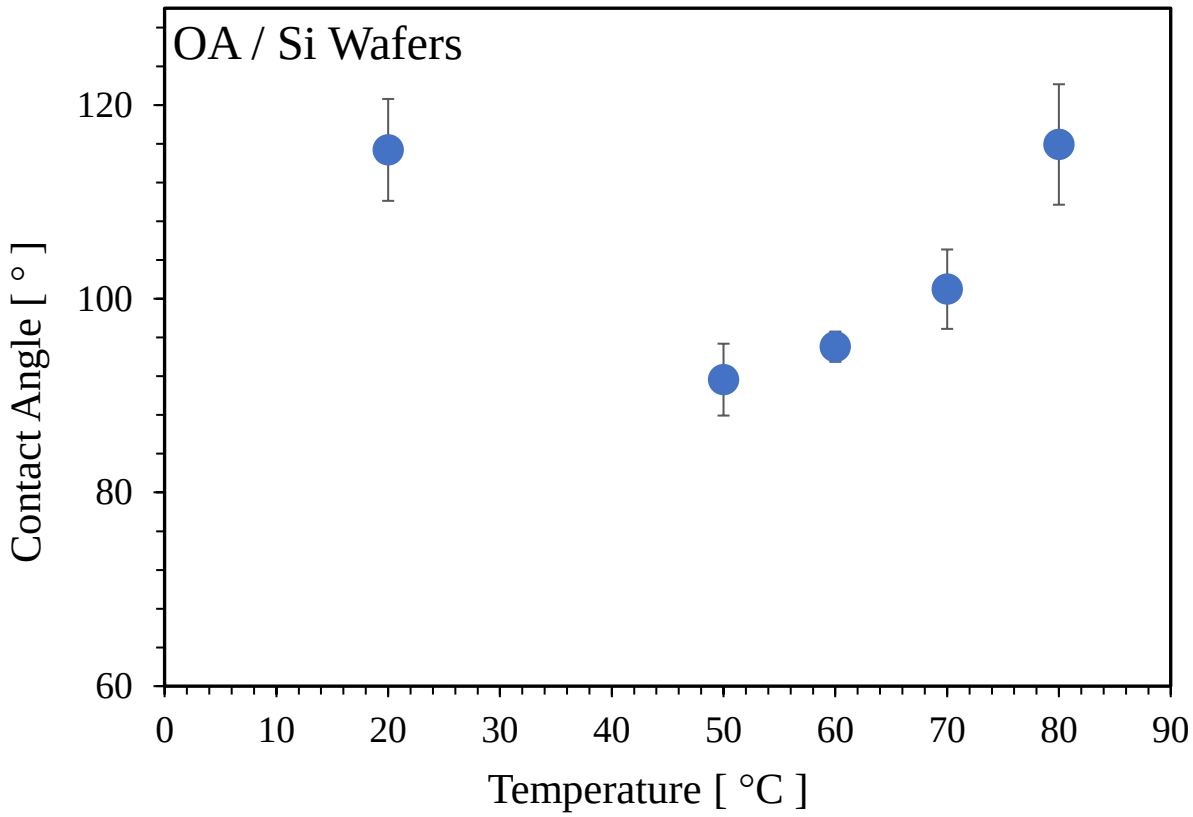

Figure 4.7 Results for contact angles of OA on Si wafers measured as a function of temperature. The data points represent 18 measurements. At room temperature the contact angle value is 115° ± 5°. The value drops to 92° ± 4° at 50 °C as temperature increases. The value remains constant at 60 °C. The value increases until it reaches 116° ± 6 at 80 °C.

on Si wafers show that maximum hydrophobicity does not increase as temperature is increased. The results do not however show that maximum hydrophobicity is independent of temperature. The second hypothesis was therefore not validated in this study. Instead, for both glass and silicon wafers, temperature appears to have a significant effect on the maximum hydrophobicity when immersion time and solution concentration are held constant.

A decrease in the contact angle as temperature increases may be due to one of two factors. Higher temperatures may cause less OA to bind to the surface in a monolayer, causing less OA to absorb in the bilayer. Alternatively, increasing temperature may cause more OA to absorb in the bilayer with the same amount of OA in the chemically absorbed monolayer. Chemical analysis of the composition of the surface will be needed to distinguish between these two possibilities.

4.4 Hypothesis Three

Hypothesis three stated that silicon oxide-like surfaces that are functionalized with a wet chemistry solution of SA between room temperature to 80 °C, above the theoretical minimum concentration, Cm, and at the optimal functionalization time have a higher hydrophobicity than the same surfaces functionalized with a wet chemistry solution of OA under the same conditions. Figure 4.8 on the second next page shows comparative results for contact angles of OA and SA on glass measured as a function of temperature. The data points represent 18 measurements. For contact angle values of OA on glass, the values start at room temperature with contact angle value of 108° ± 4°. The value drops significantly to 87° ± 4° at 50 °C as temperature increases. The value increases again until it reaches 101° ± 3 at 70 °C and remains constant at 80 °C. The contact angle value for SA on glass at room temperature is 110° ± 0.2°. The value remains constant until the temperature reaches 70 °C. The value falls slightly to 98° ± 2° at 80 °C. The

graph shows that SA on glass has higher contact angle values that stay constant compared to the contact angle values for OA on glass.

Figure 4.9 on the second next page shows comparative results for contact angles of OA and SA on Si wafers measured as a function of temperature. At room temperature the contact angle value is 115° ± 5°. The value decreases significantly to 92° ± 4° at 50 °C as temperature increases. The value remains constant at 60 °C. The value starts increasing until it reaches 116° ± 6° at 80 °C. For SA on Si wafers, the values at room temperature are 117° ± 1° and remain constant over the temperature range. The graph shows that SA on Si wafers has higher hydrophobicity than OA on Si wafers over entire the temperature range.

The results in Figure 4.8 and Figure 4.9 show that SA has higher hydrophobicity than OA over most of the temperature range studied for both glass and Si wafer surfaces. The hypothesis was not validated at room temperature and for the highest temperature at 80 °C. The results inconclusively confirmed the third hypothesis that stated silicon oxide like surfaces coated with SA at temperature between room temperature and 80 °C with concentration above Cm have higher hydrophobicity than the silicon-oxides like surface coated with OA under the same condition.

The explanation observed for the differences between contact angles for OA and SA on silicon oxide like surfaces may be because SA is a saturated fatty acid with no double bond in its molecular structure, while OA is an unsaturated fatty acid possessing a double bond in the molecular structure. The molecular structure of organic acids plays an important role in the adsorption process.[37,43] Both OA and SA seem to have perpendicular and parallel orientations on the surface of silicon oxide like surface.[43] The presence of the kink shape in the cis OA makes the acid molecular structure pack less densely on the surface. The straight molecular structure

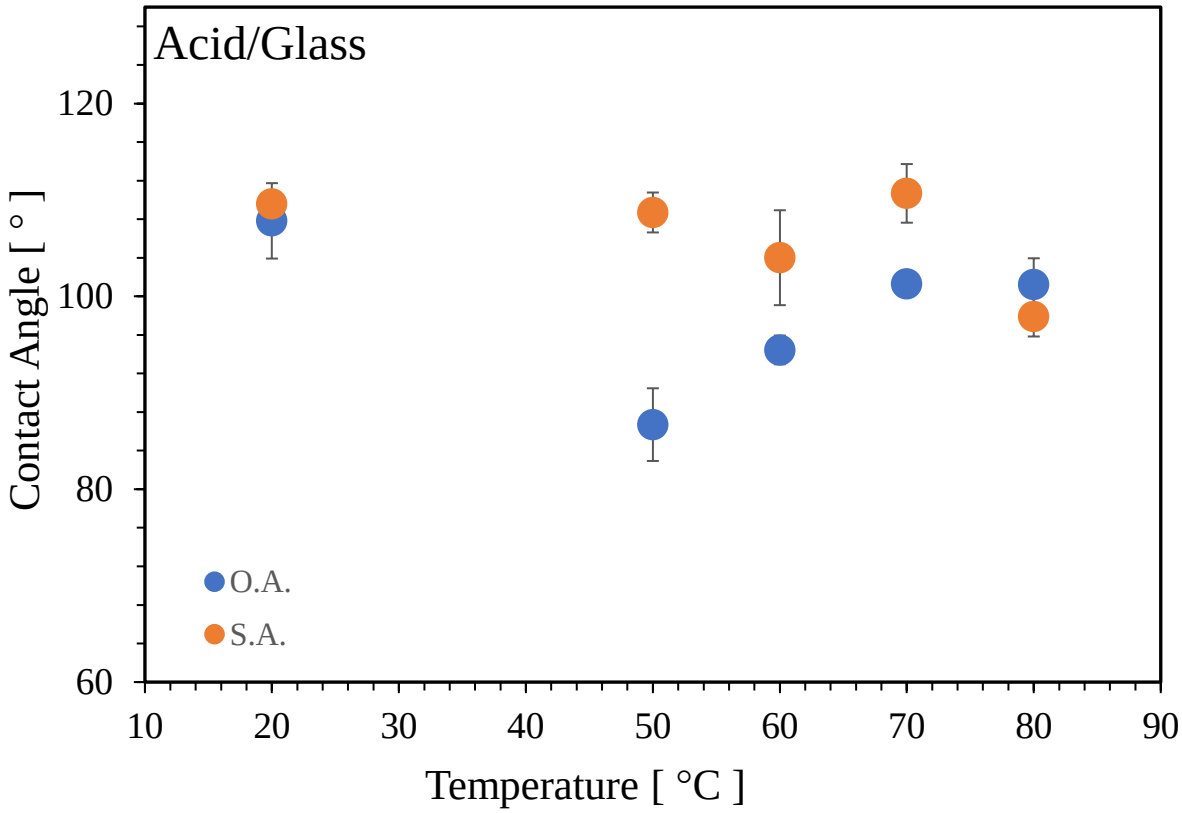

Figure 4.8 Comparative results for contact angles of OA and SA on glass measured as a function of temperature. The data points represent 18 measurements. For contact angle values of OA on glass, the values start at room temperature with contact angle value of 108 ± 4°. The value drops to 87° ± 4° at 50 °C as temperature increases. The value increases again until it reaches 101° ± 3° at 70 °C and remains constant at 80 °C. The contact angle value for SA on glass at room temperature is 110° ± 0.2°. The value remains constant until the temperature reaches 70 °C. The value falls slightly to 98° ± 2° at 80 °C.

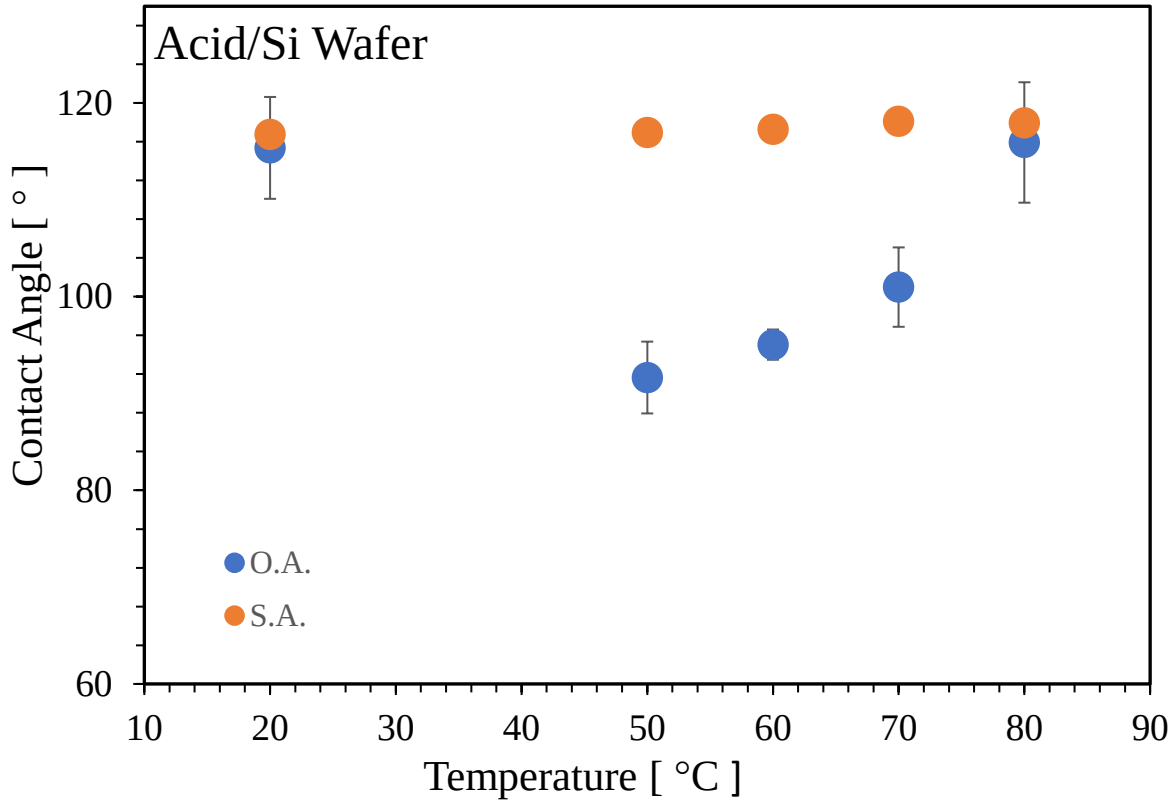

Figure 4.9 Comparative results for contact angles of OA and SA on Si wafers measured as a function of temperature. Starting at room temperature with contact angle values of 115° ± 5°. The value decreases to 92° ± 4° at 50 °C as temperature increases. The value remains constant at 60 °C. The value starts increasing until it reaches 116° ± 6° at 80 °C. For SA on Si wafers, the value at room temperature is 117° ± 1° and remain constant over the temperature range.

of SA can pack densely more on the surface.[37] By specific example from Figure 1.1, OA is shorter than SA due to the presence of the C9-C10 cis double bond. The OA molecule therefore has an intrinsic molecular rigidity, whereas the elongation of SA molecules is more strongly influenced by the crowding effects of neighboring adsorbed molecules allowing them to pack tightly.[37]

The difference in contact angle values could be due difference in surface coverage that resulted from the unsaturation in the fatty acid aliphatic group between the two type of fatty acids. This explanation was provided on previous work.[37] Under static conditions, OA was proposed to form a more compact surfactant film at low and intermediate surface coverages compared to SA. The packing efficiency may have been influenced by the packing structure at the surface. At high surface coverage, the study showed film properties of OA and SA becoming more similar. Additionally, the unsaturation causes OA molecules to adopt slightly more upward conformations than SA molecules.

Both Figures 4.8 and 4.9 respectively for SA on glass and SA on Si wafers show that maximum hydrophobicity does not increase as temperature is increased. The results show that maximum hydrophobicity is independent of temperature with SA on glass or on silicon wafers at room temperature. For SA on silicon wafers, temperature appears to have no effect on maximum hydrophobicity when immersion time and concentration are kept constant. For SA on glass, temperature appears to also have no effect on the maximum hydrophobicity when immersion time and solution concentration are held constant. Temperature increase with SA may cause the bilayer to be removed and to bind to the surface as a monolayer, causing the surface maximum hydrophobicity to be less affected with the temperature increase. The chemical structure of SA may be responsible of SA being thermodynamically less impacted by temperature. Chemical

analysis of the composition of the surfaces will be needed to determine the exact thermodynamic impact of OA and SA molecular structures on silicon oxide like surfaces.

4.5 Summary

The results demonstrated conclusively that glass and silicon wafer surfaces can be functionalized with oleic acid or steric acid using wet chemistry methods. Mica could however not be consistently functionalized with the same procedures. The organic acid solution appears to etch the mica surfaces.

Functionalizing with oleic acid at room temperature required at least 1,000 min on both surfaces of glass and Si wafers. Contact angles for oleic acid on glass reached a maximum of 108 ± 4° at 1,000 min and decreased back to 63 ± 5° for any longer times. Contact angles for oleic acid on glass reached a maximum of 115 ± 5° at 1,000 min and decreased back to 65 ± 5° for any longer times.

Stearic acid on Si wafers had a higher maximum contact angle than on glass over temperature from room temperature to 80°C. Contact angles for stearic acid and oleic acid on glass and Si wafers are statistically the same at room temperature and at 80°C. Stearic acid has higher maximum contact angle from 50 °C to 70 °C than oleic acid on both glass and Si wafers.

Chapter 5. Summary, Conclusions, and Future Work

5.1 Summary

The goal for this study was to determine the best preparation steps to functionalize hydrophilic silicon oxide-like surfaces hydrophobic using fatty acids with a wet chemistry method. Surfaces of mica, glass, and oxidized Si wafer were immersed in solutions of oleic acid (OA) and stearic acid (SA) in wet chemistry method. The cleaning method, and solution concentration were kept constant. Functionalization time and temperature were varied.

This study had three hypotheses. The first hypothesis was that an optimal reaction time exists to obtain a maximum hydrophobicity for the silicon oxide - like surfaces using wet chemistry deposition of OA at a concentration well enough above a theoretical minimum, Cm. The second hypothesis was that the maximum degree of hydrophobicity for silicon oxide-like surfaces is independent of the temperature solutions of OA at the optimal functionalization time and above concentration Cm. The final hypothesis was that silicon oxide-like surfaces that are functionalized with a wet chemistry solution of SA between room temperature to 80 °C, above Cm, and at the optimal functionalization time have a higher hydrophobicity than the same surfaces functionalized with a wet chemistry solution of OA under the same conditions.

Glass substrates were cleaned using a 30 min immersion in 1:1 MeOH / HCl solution followed by a H_2SO_4 treatment, and an ethanol rinse and bath. Samples were immersed in organic acids solutions of 0.28 mM at various functionalization times and various temperatures,

then dried at 150 °C overnight before characterization. Silicon wafers samples were cleaned with standard cleaning solution one (SC1) and standard cleaning solution two (SC2) cleaning at 80 °C followed with an ethanol rinse and bath. The samples were immersed in organic acids solutions of 0.28 mM for various functionalization times and temperatures, and then dried overnight at 150 °C before characterization.

Contact angle were compiled and analyzed as a function of time and as a function of temperature. Measurements were made at three different locations on all substrates (glass and Si wafers), and the experiments were repeated six times for each variation in condition (time and temperature). Unweighted averages and standard uncertainties in contact angle were calculated from the resulting 18 data points.

5.2 Conclusions

The results demonstrated conclusively that glass and silicon wafer surfaces can be functionalized with OA or SA using wet chemistry methods. Mica could however not be consistently functionalized with the same procedures. The organic acid solution appeared to etch the mica surface.

The first hypothesis was validated. A maximum hydrophobicity exists for OA on glass and oxidized Si wafers. The hydrophilic silicon-oxides like surfaces can be made hydrophobic. The maximum hydrophobicity is at 1,000 min functionalization time. After reaching the maximum hydrophobicity the contact angle values show an abrupt decrease, rendering the surfaces hydrophilic again for immersion times above 1,000 min. The conclusion drawn is that the carboxylic groups in OA create a chemical – physical bilayer after 1,00 min. The formation of the bilayer is proposed to be due to using excess of OA. The concentration C 100 x times a

theoretical minimum is enough to create a micelle bilayer. The conclusion is consistent with literature reports of bilayers in similar systems with OA.

The second hypothesis was not validated. As the temperature of OA solution increased, the maximum hydrophobicity initially decreased. Increasing temperature could cause destruction of the bilayer.

The third hypothesis was inconclusively validated. Stearic acid coated glass or oxidized Si wafer surfaces have higher contact angles than OA coated surfaces only at temperatures above room temperature or below 80 °C. The explanation proposed is that SA is a saturated fatty acid with no double bond in its molecular structure and OA is an unsaturated fatty acid therefore possessing double bond in the molecular structure. The presence of the kink in the cis OA makes the acid molecular structure pack less on the surface. Oleic acid is more affected by the thermodynamics caused by temperature change than SA.

5.3 Future Work

The questions that arose from this study can be framed as hypotheses for future work proposals. Three significant considerations are identified. One deals with functionalizing mica. The other two address the possibility of bilayers with OA or SA.

A first hypothesis that can be study for future work is that mica can be successfully functionalized with vapor deposition of oleic acid or stearic acid. Vapor deposition involves exposing a surface to a vapor of the acid, typically by placing the sample in a closed container suspended above the heated liquid. The approach is to vary temperature, and functionalization time. The metric for success is to make hydrophilic mica surfaces hydrophobic. The validity is proven using a graph of contact angle versus temperature or time, with all other factors staying

constant. The first hypothesis will be true if contact angle reaches maximum hydrophobicity value within a certain temperature or time.

A second hypothesis for future work is to establish that oleic acid forms bilayer on glass or oxidized Si wafer surfaces under high solution concentrations. One significant expectation is that using lower acid concentrations will avoid the formation of a bilayer. The experiment should therefore vary the solution concentration as parameter with all other parameters hold constant. Experimental work will be conducted with a serial dilutions to create lower concentrations. The validity of the second hypothesis can be tested using a graph of contact angle versus concentration, with all other factors staying constant. A bilayer will be strongly indicated if contact angle plateaus at a maximum value within concentrations below the theoretical minimum concentration and does not decrease with increasing functionalization time. All the previous characterization method applies.

A final hypothesis for future work is that stearic acid does not form a bilayer under the same conditions where oleic acid does form a bilayer. The approach for this study is to repeat the experiments where the bilayer is proposed to form with oleic acid but use stearic acid instead. All other aspects of the characterization method will apply.

Additional studies can include other characterization techniques. One of those is infra-red spectroscopy with an attenuated total reflectance mode (ATR). The intent was to find the acid peaks on the surface. The studies were unsuccessful. We believed that we were unsuccessful because the sensitivity of the ATR was too low to detect the molecules on the surface. Perhaps the sensitivity could be increased by other modes. Another characterization technique to consider is x-ray photoelectron spectroscopy (XPS). In fact, references in the background section reported that XPS was used to study surfaces functionalized with oleic acid. This method will prove

useful to determine the coverage on the surface. Finally, atomic force microscopy could be used. Atomic force microscopy technique determines the packing on a surface at atomic resolution. This technique will be especially useful on the atomically smooth mica smooth surfaces.

References

(1) Rosales, A.; Esquivel, K. SiO2@TiO2 Composite Synthesis and Its Hydrophobic Applications: A Review. *Catalysts* **2020**, *10* (2), 171. https://doi.org/10.3390/catal10020171.

(2) Hamzah, A. A.; Nadzirah, Sh. Biosensor Development. In *Encyclopedia of Sensors and Biosensors*; Elsevier, 2023; pp 209–217. https://doi.org/10.1016/B978-0-12-822548-6.00112-6.

(3) Neffe, A. T.; Julich-Gruner, K. K.; Lendlein, A. Combinations of Biopolymers and Synthetic Polymers for Bone Regeneration. In *Biomaterials for Bone Regeneration*; Elsevier, 2014; pp 87–110. https://doi.org/10.1533/9780857098104.1.87.

(4) Matl, F. D.; Zlotnyk, J.; Obermeier, A.; Friess, W.; Vogt, S.; Büchner, H.; Schnabelrauch, H.; Stemberger, A.; Kühn, K.-D. New Anti-Infective Coatings of Surgical Sutures Based on a Combination of Antiseptics and Fatty Acids. *J. Biomater. Sci. Polym. Ed.* **2009**, *20* (10), 1439–1449. https://doi.org/10.1163/092050609X12457418973107.

(5) Vijay, N.; Morris, M. Role of Monocarboxylate Transporters in Drug Delivery to the Brain. *Curr. Pharm. Des.* **2014**, *20* (10), 1487–1498. https://doi.org/10.2174/13816128113199990462.

(6) Gonzalez-Pech, N. I.; Grassian, V. H. Surface Chemical Functionalities of Environmental Nanomaterials. In *Encyclopedia of Interfacial Chemistry*; Elsevier, 2018; pp 817–828. https://doi.org/10.1016/B978-0-12-409547-2.13188-9.

(7) Farsi, M. CO2 Capture by Solvents Modified with Nanoparticles. In *Advances in Carbon Capture*; Elsevier, 2020; pp 107–123. https://doi.org/10.1016/B978-0-12-819657-1.00005-0.

(8) Liu, Y.; Liu, Y.; Tang, L.; Zhou, Y.; Yang, G.; Zeng, G.; Liu, H. Mesoporous Carbon-Based Composites for Adsorption of Heavy Metals. In *Nanohybrid and Nanoporous Materials for Aquatic Pollution Control*; Elsevier, 2019; pp 63–102. https://doi.org/10.1016/B978-0-12-814154-0.00003-7.

(9) Loy, D. A. Sol–Gel Processing. In *Encyclopedia of Physical Science and Technology*; Elsevier, 2003; pp 257–276. https://doi.org/10.1016/B0-12-227410-5/00697-9.

(10) Johansson, K. Plasma Modification of Natural Cellulosic Fibres. In *Plasma Technologies for Textiles*; Elsevier, 2007; pp 247–281. https://doi.org/10.1533/9781845692575.2.247.

(11) Vossen, J. *Physics of Thin Films*; 1977; Vol. 9.

(12) Goyal, S. Silanes: Chemistry and Applications. *J. Indian Prosthodont. Soc.* **2006**, *6* (1), 14. https://doi.org/10.4103/0972-4052.25876.

(13) Štiglic, A. D.; Gürer, F.; Lackner, F.; Bračič, D.; Winter, A.; Gradišnik, L.; Makuc, D.; Kargl, R.; Duarte, I.; Plavec, J.; Maver, U.; Beaumont, M.; Kleinschek, K. S.; Mohan, T. Organic Acid Cross-Linked 3D Printed Cellulose Nanocomposite Bioscaffolds with Controlled Porosity, Mechanical Strength, and Biocompatibility. *iScience* **2022**, *25* (5), 104263. https://doi.org/10.1016/j.isci.2022.104263.

(14) Choi, H.; Nguyen, P. T.; In, J. B. Laser Transmission Welding and Surface Modification of Graphene Film for Flexible Supercapacitor Applications. *Appl. Surf. Sci.* **2019**, *483*, 481–488. https://doi.org/10.1016/j.apsusc.2019.03.349.

(15) Parvate, S.; Dixit, P.; Chattopadhyay, S. Superhydrophobic Surfaces: Insights from Theory and Experiment. *J. Phys. Chem. B* **2020**, *124* (8), 1323–1360. https://doi.org/10.1021/acs.jpcb.9b08567.

(16) Shanmugam, N.; Pugazhendhi, R.; Madurai Elavarasan, R.; Kasiviswanathan, P.; Das, N. Anti-Reflective Coating Materials: A Holistic Review from PV Perspective. *Energies* **2020**, *13* (10), 2631. https://doi.org/10.3390/en13102631.

(17) Law, A. M.; Jones, L. O.; Walls, J. M. The Performance and Durability of Anti-Reflection Coatings for Solar Module Cover Glass – a Review. *Sol. Energy* **2023**, *261*, 85–95. https://doi.org/10.1016/j.solener.2023.06.009.

(18) Yu, Z.; Du, X.; Zhu, P.; Zhao, T.; Sun, R.; Chen, J.; Wang, N.; Li, W. Surface Modified Hollow Glass Microspheres-Epoxy Composites with Enhanced Thermal Insulation and Reduced Dielectric Constant. *Mater. Today Commun.* **2022**, *32*, 104046. https://doi.org/10.1016/j.mtcomm.2022.104046.

(19) Calovi, M.; Rossi, S. Durability and Thermal Behavior of Functional Paints Formulated with Recycled-Glass Hollow Microspheres of Different Size. *Materials* **2023**, *16* (7), 2678. https://doi.org/10.3390/ma16072678.

(20) Li, Z.; Zhu, Y. Surface-Modification of SiO2 Nanoparticles with Oleic Acid. *Appl. Surf. Sci.* **2003**, *211* (1–4), 315–320. https://doi.org/10.1016/S0169-4332(03)00259-9.

(21) Yao, J.; Zhong, L.; Natelson, D.; Tour, J. M. Silicon Oxide: A Non-Innocent Surface for Molecular Electronics and Nanoelectronics Studies. *J. Am. Chem. Soc.* **2011**, *133* (4), 941–948. https://doi.org/10.1021/ja108277r.

(22) Fopase, R.; Paramasivam, S.; Kale, P.; Paramasivan, B. Strategies, Challenges and Opportunities of Enzyme Immobilization on Porous Silicon for Biosensing Applications. *J. Environ. Chem. Eng.* **2020**, *8* (5), 104266. https://doi.org/10.1016/j.jece.2020.104266.

(23) Macfarlane, A.; Martin, G. A World of Glass. *Science* **2004**, *305* (5689), 1407–1408. https://doi.org/10.1126/science.1093597.

(24) Ji, X.; Wang, W.; Duan, J.; Zhao, X.; Wang, L.; Wang, Y.; Zhou, Z.; Li, W.; Hou, B. Developing Wide pH-Responsive, Self-Healing, and Anti-Corrosion Epoxy Composite Coatings Based on Encapsulating Oleic Acid/2-Mercaptobenzimidazole Corrosion Inhibitors in Chitosan/Poly(Vinyl Alcohol) Core-Shell Nanofibers. *Prog. Org. Coat.* **2021**, *161*, 106454. https://doi.org/10.1016/j.porgcoat.2021.106454.

(25) Nogues, C.; Wanunu, M. A Rapid Approach to Reproducible, Atomically Flat Gold Films on Mica. *Surf. Sci.* **2004**, *573* (3), L383–L389. https://doi.org/10.1016/j.susc.2004.10.019.

(26) Pan, X.; Li, S.; Li, Y.; Guo, P.; Zhao, X.; Cai, Y. Resource, Characteristic, Purification and Application of Quartz: A Review. *Miner. Eng.* **2022**, *183*, 107600. https://doi.org/10.1016/j.mineng.2022.107600.

(27) Asem A. Atia, Ahmed M. El-Nahas, Asmaa M. Marie and Laila D. Al Mahdy. Adsorption of Oleic Acid on Silica Gel Derived from Rice Ash Hulls: Experimental and Theoretical Studies. *Asem Atia AlAdsorption Sci. Technol. Vol 24 No 9 2006 Asem A. Atia et al./Adsorption Science&Technology Vol. 24 No. 9 2006*.

(28) De Poel, W.; Pintea, S.; Drnec, J.; Carla, F.; Felici, R.; Mulder, P.; Elemans, J. A. A. W.; Van Enckevort, W. J. P.; Rowan, A. E.; Vlieg, E. Muscovite Mica: Flatter than a Pancake. *Surf. Sci.* **2014**, *619*, 19–24. https://doi.org/10.1016/j.susc.2013.10.008.

(29) L.T. Zhura6le6 / Colloids and Surfaces A: Physicochem. Eng. Aspects 173 (2000) 1–38. The Surface Chemistry of Amorphous Silica. Zhuravlev Model L.T. Zhuravlev.

(30) Zaccone, A.; Blundell, J. R.; Terentjev, E. M. Network Disorder and Nonaffine Deformations in Marginal Solids. *Phys. Rev. B* **2011**.

(31) Doussal, P. L. Moving Glass Theory of Driven Lattices with Disorder.

(32) Kargozar, S.; Kermani, F.; Mollazadeh Beidokhti, S.; Hamzehlou, S.; Verné, E.; Ferraris, S.; Baino, F. Functionalization and Surface Modifications of Bioactive Glasses (BGs): Tailoring of the Biological Response Working on the Outermost Surface Layer. *Materials* **2019**, *12* (22), 3696. https://doi.org/10.3390/ma12223696.

(33) Lee, D. H.; Condrate, R. A.; Lacourse, Sr., W. C. FTIR Spectral Chacterization of Thin Film Coatings of Oleic Acid on Glasses: Part II Coatings on Glass from Different Media Such as Water, Alcohol, Benzene and Air. *J. Mater. Sci.* **2000**, *35* (19), 4961–4970. https://doi.org/10.1023/A:1004890627405.

(34) Parfitt, G. D. SURFACE CHEMISTRY OF OXIDES. In *Colloid and Surface Science*; Elsevier, 1977; pp 415–418. https://doi.org/10.1016/B978-0-08-021570-9.50008-5.

(35) Ciampi, S.; Harper, J. B.; Gooding, J. J. Wet Chemical Routes to the Assembly of Organic Monolayers on Silicon Surfaces via the Formation of Si–C Bonds: Surface Preparation, Passivation and Functionalization. *Chem. Soc. Rev.* **2010**, *39* (6), 2158. https://doi.org/10.1039/b923890p.

(36) Bahuleyan, B. K.; Toussaint, K.; Rinnert, H.; Vallon, R.; Molinari, M.; Chuburu, F.; Cadiou, C. Silicon Wafer Functionalization with a Luminescent Tb(III) Coordination Complex: Synthesis, Characterization, and Application to the Optical Detection of NO in the Gas Phase. *Molecules* **2019**, *24* (10), 1914. https://doi.org/10.3390/molecules24101914.

(37) Doig, M.; Warrens, C. P.; Camp, P. J. Structure and Friction of Stearic Acid and Oleic Acid Films Adsorbed on Iron Oxide Surfaces in Squalane. *Langmuir* **2014**, *30* (1), 186–195. https://doi.org/10.1021/la404024v.

(38) Hada, D.; Rathore, K.; Chauhan, N. P. S.; Sharma, K.; Mozafari, M. Functional Protein to Polymer Surfaces: An Attachment. In *Advanced Functional Polymers for Biomedical*

Applications; Elsevier, 2019; pp 191–210. https://doi.org/10.1016/B978-0-12-816349-8.00010-2.

(39) Honciuc, A. Surfactants and Amphiphiles. In *Chemistry of Functional Materials Surfaces and Interfaces*; Elsevier, 2021; pp 43–77. https://doi.org/10.1016/B978-0-12-821059-8.00011-9.

(40) Abesekara, M. S.; Chau, Y. Recent Advances in Surface Modification of Micro- and Nano-Scale Biomaterials with Biological Membranes and Biomolecules. *Front. Bioeng. Biotechnol.* **2022**, *10*, 972790. https://doi.org/10.3389/fbioe.2022.972790.

(41) Simopoulos, A. P. The Importance of the Ratio of Omega-6/Omega-3 Essential Fatty Acids. *Biomed. Pharmacother.* **2002**, *56* (8), 365–379. https://doi.org/10.1016/S0753-3322(02)00253-6.

(42) Prieto Vidal, N.; Adeseun Adigun, O.; Pham, T.; Mumtaz, A.; Manful, C.; Callahan, G.; Stewart, P.; Keough, D.; Thomas, R. The Effects of Cold Saponification on the Unsaponified Fatty Acid Composition and Sensory Perception of Commercial Natural Herbal Soaps. *Molecules* **2018**, *23* (9), 2356. https://doi.org/10.3390/molecules23092356.

(43) Rezaei Gomari, K. A.; Denoyel, R.; Hamouda, A. A. Wettability of Calcite and Mica Modified by Different Long-Chain Fatty Acids (C18 Acids). *J Colloid Interface Sci* **2006**, *297* (2), 470–479. https://doi.org/10.1016/j.jcis.2005.11.036.

(44) Lee, D. H.; Condrate Sr., R. A. FTIR Spectral Characterization of Thin Film Coatings of Oleic Acid on Glasses: I. Coatings on Glasses from Ethyl Alcohol. *J. Mater. Sci.* **1999**, *34* (1), 139–146. https://doi.org/10.1023/a:1004494331895.

(45) Ferlenda, G.; Cazzola, M.; Ferraris, S.; Cochis, A.; Kumar, A.; Prenesti, E.; Spriano, S.; Vernè, E. Surface Functionalization of a Silica-Based Bioactive Glass with Compounds

from *Rosa Canina* Bud Extracts. *ACS Biomater. Sci. Eng.* **2021**, *7* (1), 96–104. https://doi.org/10.1021/acsbiomaterials.0c01170.

(46) Parker, J. L.; Cho, D. L.; Claesson, P. M. Plasma Modification of Mica: Forces between Fluorocarbon Surfaces in Water and a Nonpolar Liquid. *J. Phys. Chem.* **1989**, *93* (16), 6121–6125. https://doi.org/10.1021/j100353a034.

(47) Chen, B. H.; Liu, J. Z.; Shan, S. Q.; Yang, W. J. Adsorption Mechanism of Oleic Acid on the Surface of Aluminum Nanoparticle: ReaxFF Molecular Dynamics Simulation and Experimental Study. *Colloids Surf. Physicochem. Eng. Asp.* **2021**, *618*, 126500. https://doi.org/10.1016/j.colsurfa.2021.126500.

(48) Maharanwar, A.; Weimer, J. J. Analysis of the Uptake of Chlorotrimethylsilane on Glass from Toluene Solution-Phase Depositions. *Surf. Interfaces* **2017**, *7*, 29–38. https://doi.org/10.1016/j.surfin.2017.01.007.

(49) Mourougou-Candoni, N.; Thibaudau, F. Formation of Aminosilane Film on Mica. *J Phys Chem B* **2009**, *113* (39), 13026–13034. https://doi.org/10.1021/jp903021e.

(50) Bera, B. Silicon Wafer Cleaning: A Fundamental and Critical Step in Semiconductor Fabrication Process. **2019**, *5* (1).

(51) McMurry, J. *Organic Chemistry*, Ninth edition.; Cengage Learning: Boston, MA, USA, 2016.

(52) Clayden, J.; Greeves, N.; Warren, S. G. *Organic Chemistry*, 2nd ed.; Oxford University Press: Oxford ; New YorK, 2012.

(53) Kang, J.; Rowntree, P. A. Gold Film Surface Preparation for Self-Assembled Monolayer Studies. *Langmuir* **2007**, *23* (2), 509–516. https://doi.org/10.1021/la0518804.

Appendix A

Table A.1 Averages and uncertainties of 18 measurements for each of the functionalization time of OA on glass at room temperature.

Time (min)	Averages	S
1	38.72	1.69
3	51.48	6.15
10	51.69	4.12
30	44.46	3.87
100	50.89	2.88
300	56.76	3.54
600	77.82	6.54
1000	107.82	3.91
1200	54.48	5.88
3600	63.09	4.604

Table A.2 Averages and uncertainties of 18 measurements for each of the functionalization time of OA on Si wafers at room temperature.

Time (min)	Averages	S
1	37.55	1.01
3	52.28	2.48
10	52.75	3.85
30	43.94	3.76
100	51.54	2.48
300	54.42	3.35
600	55.87	3.02
1000	115.37	5.26
1200	76.29	4.39
3600	59.48	4.29

Table A.3 Averages and uncertainties of 18 measurements for OA on glass at 1,000 min functionalization time at various temperature (in °C).

Temp.	Averages	S
20	107.83	3.91
50	86.7	3.77
60	94.45	1.49
70	101.29	0.87
80	101.25	2.7

Table A.4 Averages and uncertainties of 18 measurements for OA on Si wafers at 1,000 min functionalization time at various temperature (in °C).

Temp.	Averages	S
20	115.37	5.26
50	91.65	3.71
60	95.05	1.56
70	100.99	4.099
80	115.93	6.22

Table A.5 Averages and uncertainties of 18 measurements for SA on glass at 1,000 min functionalization time at various temperature (in °C).

Temp.	Averages	S
20	109.6	0.187
50	108.7	2.071
60	104.01	4.92
70	110.68	3.04
80	97.93	2.09

Table A.6 Averages and uncertainties of 18 measurements for SA on Si wafers at 1,000 min functionalization time at various temperature (in °C).

Temp.	Averages	S
20	116.76	1.018
50	116.97	1.13
60	117.31	0.84
70	118.13	0.98
80	117.97	0.55